FLUORESCENT LABELING OF SPOCK1 AND LOCALIZATION STUDIES IN LIVE NEURAL CELL LINES

A THESIS SUBMITTED TO
THE GRADUATE SCHOOL OF NATURAL AND APPLIED SCIENCES
OF
MIDDLE EAST TECHNICAL UNIVERSITY

BY

ZEYNEP EDA KARABOĞA

IN PARTIAL FULFILLMENT OF THE REQUIREMENTS
FOR
THE DEGREE OF MASTER OF SCIENCE
IN
BIOLOGY

NOVEMBER 2022

Approval of the thesis:

FLUORESCENT LABELING OF SPOCK1 AND LOCALIZATION STUDIES IN LIVE NEURAL CELL LINES

submitted by **Zeynep Eda Karaboğa** in partial fulfillment of the requirements for the degree of **Master of Science** i**n Biology, Middle East Technical University** by,

Prof. Dr. Halil Kalıpçılar
Dean, Graduate School of **Natural and Applied Sciences** _____

Prof. Dr. Ayşe Gül Gözen
Head of the Department, **Biology** _____

Assoc. Prof. Dr. Çağdaş Devrim Son
Supervisor, **Biology, METU** _____

Assoc. Prof. Dr. Yeşim Aydın Son
Co-Supervisor, **Medical Informatics, METU** _____

Examining Committee Members:

Prof. Dr. Sreeparna Banerjee
Biology, METU _____

Assoc. Prof. Dr. Çağdaş Devrim Son
Biology, METU _____

Assoc. Prof. Dr. Tülin Yanık
Biology, METU _____

Assoc. Prof. Dr. Özgül Persil Çetinkol
Chemistry, METU _____

Assoc. Prof. Dr. Gamze Bora
Medical Biology, Hacettepe University _____

Date: 30.11.2022

I hereby declare that all information in this document has been obtained and presented in accordance with academic rules and ethical conduct. I also declare that, as required by these rules and conduct, I have fully cited and referenced all material and results that are not original to this work.

Name Last Name: Zeynep Eda Karaboğa

Signature :

ABSTRACT

FLUORESCENT LABELING OF SPOCK1 AND LOCALIZATION STUDIES IN LIVE NEURAL CELL LINES

Karaboğa, Zeynep Eda
Master of Science, Biology
Supervisor: Assoc. Prof. Dr. Çağdaş Devrim Son
Co-Supervisor: Assoc. Prof. Dr. Yeşim Aydın Son

November 2022,84 pages

Alzheimer's disease is the most common form of dementia and is incurable. The late-onset Alzheimer's disease (LOAD) is associated with complex genetic transition, and the molecular background has not been enlightened yet. Our previous research on the meta-analysis of genome-wide association studies (GWAS) showed a statistical correlation between SPOCK1 variants and LOAD. Also, it is co-regulated with apolipoprotein (APP), one of the proteins clinically linked with LOAD. Furthermore, the SPOCK1 protein recently had considerable attention due to its role in cell adhesion in various cancers. Considering the current literature on SPOCK1, we hypothesized that SPOCK1 might impact Alzheimer's pathogenesis in neural cells. In this study, human neuroblastoma and astroglia cells expressing fluorescent tagged SPOCK1 were constructed to study the expression and localization of SPOCK1. IHC and confocal image analysis with various organelle labels were performed, and co-localization data showed SPOCK1 localized in mitochondria for both neuroblastoma and astroglial cells. The data obtained in this study related to the localization of SPOCK1 *in vitro*

could contribute to the research of the molecular background of Alzheimer's disease in the future.

Keywords: SPOCK1 Gene and Protein, LOAD, Neural Cell Lines

ÖZ

CANLI SİNİR HUCRE HATLARINDA SPOCK1'IN FLORESAN İŞARETLENMESİ VE LOKALİZASYONU

Karaboğa, Zeynep Eda
Yüksek Lisans, Biyoloji
Tez Yöneticisi: Doç. Dr. Çağdaş Devrim Son
Ortak Tez Yöneticisi: Doç. Dr. Yeşim Aydın Son

Kasım 2022, 84 sayfa

Alzheimer hastalığı demansın tedavi edilemeyen en yaygın şeklidir. Geç başlangıçlı Alzheimer hastalığı (LOAD) karmaşık genetik ile ilişkilidir ve moleküler arka planı henüz aydınlatılamamıştır. Genom çapında ilişkilendirme çalışmalarının (GWAS) meta-analizine ilişkin önceki araştırmamız, SPOCK1 varyantları ile LOAD arasında istatiksel bir korelasyonu ortaya koydu. Ayrıca klinik olarak LOAD ile bağlantılı proteinlerden biri olan apolipoprotein (APP) ile birlikte regülasyonu mevcuttur. Aynı zamanda SPOCK1 proteini, çeşitli kanserlerde hücre yapışmasındaki rolü nedeniyle son zamanlarda dikkat çekici bir konu haline gelmiştir. SPOCK1 ile ilgili mevcut literatür göz önüne alındığında SPOCK1'ın nöral hücrelerde Alzheimer patogenezini etkiyebileceğini düşünmekteyiz.Bu çalışmada, SPOCK1'in hücre ekspresyonunu ve lokalizasyonunu incelemek için floresan işaretlemeli SPOCK1'i insan nöroblastoma ve astroglia hücreleri kullanılarak çalışmalar yapıldı. Çeşitli organel işaretlemeleri ile IHC ve konfokal görüntü analizi yapıldı. İşaretli SPOCK1 proteinleri, işaretlenmemiş/normal proteinlerle ekspresyon ve hücre içi yerleşimleri açısından karşılaştırılmıştır. Çeşitli organel belirteçleri ile iki ayrı hücre hattında konfokal görüntülemeler gerçekleştirildikten sonra SPOCK1'in mitokondride lokalize olduğu bulunmuştur. SPOCK1'in *in vitro* lokalizasyonu ile ilgili bu çalışmada elde edilen

veriler, gelecekte Alzheimer hastalığının moleküler altyapısının araştırılmasına katkı sağlayabilir.

Anahtar Kelimeler: SPOCK1 Gen ve Proteini, LOAD, Sinir Hücresi

To my family.

ACKNOWLEDGMENTS

First of all, I wish to express my sincere gratitude to my beloved advisors Assoc. Prof. Dr. Yeşim Aydın Son and Assoc. Prof. Dr. Çağdaş Devrim Son for their patience, counsel, advice, criticism, encouragement, and insight during the research. It was a wonderful opportunity and such an amazing field of study. I am grateful to them for their fairness and helpfulness to their students. I am grateful, and I owe them a lot for endless moral support, guidance, and tolerance. For the rest of my life, I will be forever thankful to them not only academically but also for their perspectives. I could not have chosen better advisors! Secondly, I would like to thank the best tutor Dr.Tugba Dursun Usal, for her endless guidance, moral support, discipline, and tolerance. I appreciate finding a chance to work under her supervision. I owe her a lot for being my idol for both my scientific career and my entire life because, without her, I would have to continue my academic career without an idol. She will always have my gratitude for the rest of my life. I would like to thank the examining committee; for their invaluable suggestions to complete this study. Also, special thanks to İrem Aydın for being such an amazing lab mate and friend. I will always remember how dedicated you are. I appreciate the time you took out of your busy schedule to help me several times. I would like to thank Orkun Cevheroğlu and Son-Lab Kök Hücre Team for their guidance and support. I am grateful to Berkay Demirbaş and Saeed for their guidance and endless mental and scientific support. I will always be grateful to them for my entire academic life. I want to thank all old and new SON Lab members for believing in me to complete this study and giving me support.

I would like to thank my cheerleader whose support I always feel in my heart no matter how far away Tamara Ecem Korkut, my confidant Buse Çelikkoparan, my comforting friend Serenay Boz, my warm-hearted friend Nilay İnce Yıldız, my little brother Umut Barış Korkut, my comrade Kutay Şendil, my logical friend Sercan Tekin, my reliable friend Kaan Topçu, my ambitious friend Erekol Zeren, my dynamic friend Oğuz Demet, my loyal friend Buket Güner, my empathetic friend Çağrı Tunca, my helpful friend Uğurcan Mandacı and my energetic friend Gizem Kaya for their endless

patience and support. Also, I am thankful to my dearest Hikmet Çom for being so supportive, so understanding, and for being such a great friend.

Moreover, I would like to extend my sincere thanks to my precious employers Dr. Burcu Sağlam Ada, Dr. Ayşe Nur Kavasoğlu, Okan Özdemir, Berk Özdemir, Özgür Incekara, Mehmet Mandacı, and Incekaralar family for their patience, guidance, moral and material support. Even though they're not physically with me, I feel their support and encouragement.

Most importantly, I am thankful for my life-saver mother Hanife Karaboğa, my compassionate father, Aslan Karaboğa, my gracious sister Buse Ece Karaboğa and my little paw sister Güneş for their endless support and help. I consider myself extremely privileged to have such a family. I am dedicating all my achievements to my family.

TABLE OF CONTENTS

APPENDICES

LIST OF TABLES

LIST OF FIGURES

LIST OF ABBREVIATIONS

AD	Alzheimer's Disease
apoE	Apolipoprotein E
APP	Amyloid Precursor Protein
CSF	Cerebrospinal Fluid
CNS	Central Nervous System
D-MEM	Dulbecco's Modified Eagle Medium
DMSO	Dimethyl sulfoxide
DNA	Deoxyribonucleic Acid
ECM	Extracellular Matrix
EMEM	Eagle's Minimal Essential Medium
FBS	Fetal Bovine Serum
GAG	Glycosaminoglycan
GFP	Green Fluorescent Protein
IHC	Immunohistochemistry
kb	Kilo Base Pair
LB	Luria Bertani
LOAD	Late On-Set Alzheimer's Disease
mCherry	Monomeric Cherry
PBS	Phosphate Buffered Saline
PCR	Polymerase Chain Reaction
SPARC	Secreted Protein Acidic and Cystine Rich
SPOCK1	SPARC (Osteonectin), Cwcv And Kazal Like Domains Proteoglycan 1

CHAPTER 1

INTRODUCTION

Alzheimer's disease is a progressive, degenerative disorder that affects the brain and results in impaired memory, thinking, and behavior. It is the most common form of dementia, is incurable, and progresses very insidiously, causing difficulties for patients and their relatives. There is currently no cure for Alzheimer's disease, but there are treatments that may alleviate symptoms (Kuhar *et al.*, 2022).

Early onset (before age 65) of the disease is less frequent and occurs in less than 10% of all Alzheimer's patients. The prevalence of late-onset Alzheimer's disease (LOAD) is estimated to be between 5-8% in people over 65 and up to 50% in people over 85.(Mendez, 2017) Early onset Alzheimer's disease shows familial inheritance, so have a genetic component, with specific genes increasing the risk of developing the disease. However, environmental factors, such as lifestyle and diet, may also play a role. The late-onset Alzheimer’s disease (LOAD) is associated with complex genetic transition, and the molecular background has not been enlightened yet(Perez *et al*. 2014).

Our group's research on genome-wide association studies (GWAS) meta-analysis revealed a statistical relationship between SPOCK1 variants and LOAD. SPOCK1 protein has recently received much attention due to its possible co-regulation with apolipoprotein (APP), a well-known protein clinically linked with Alzheimer's Disease.

While results of our previous study showed that SPOCK1 could be associated with Late-onset Alzheimer’s disease, in the literature, the function of this protein has not been fully explained or correlated with LOAD. The currently available research on SPOCK1 and the nervous system suggests the presence of the SPOCK1 mRNA in the brain, retina, spinal cord, and the developing central nervous system (O'Brown *et al*., 2021).

The lack of molecular and functional data on SPOCK1 in neural cells led us to design a study to reveal its possible function(s). Understanding the role of SPOCK1 in neural cells can reveal new insight into AD pathogenesis, leading to new diagnostic and therapeutic approaches. For this purpose, our main aim is to identify the expression pattern and the localization of the SPOCK1 protein in various neural cells.

To identify the intracellular localization of SPOCK1, human neuroblastoma and astroglia cells expressing fluorescent tagged SPOCK1 were constructed and imaged using a confocal microscope. For this purpose, we transfected fluorescent-tagged SPOCK1 with various organelle markers. The expression patterns of the tagged SPOCK1 proteins were confirmed with IHC studies. The antibody staining is used for labeling wild-type SPOCK1 protein, which co-localized with the tagged constructs in the two neural cell lines used in this study. The mitochondrial localization of the SPOCK1 in neural cells has been observed for the first time in this study.

A recent immunohistochemistry study in hepatoma cell lines also showed that SPOCK1 is located at mitochondria. This study concluded that the mitochondrial distribution suggests SPOCK1 may have an unknown physiological role in healthy hepatocytes (Váncza *et al.*, 2022). This localization study was essential to identifying SPOCK1's unknown function(s) in hepatocytes. Thus, our findings throughout this thesis work could shed some light on the research for diagnosing and treating AD by making it possible to hypothesize new functions based on the intracellular localization of the gene product.

CHAPTER 2

LITERATURE REVIEW

2.1 Nervous Systems

The central nervous system comprises the spinal cord and the brain (CNS). The three primary functions of the CNS are receiving sensory data, interpreting it, and transmitting motor impulses. The CNS controls how the body responds by receiving sensory data from the neurological system. The central nervous system's main job is to receive information from various bodily regions and coordinate this activity to cause the body to respond. Since the neuron is the fundamental building block of the nervous system, most neurologic disorders must ultimately involve malfunctioning neurons. The three main components of the CNS are the brain, spinal cord, and neurons (or nerve cells). Each of the three CNS components, which cooperate in interpreting information and control how the body responds, is essential to how the body functions. Figure 2.1 shows an illustration of CNS & PNS. In conventional histology, the "neuron" refers to the cell body of the nerve cell, which typically only makes up a small fraction of the total cell volume. The cell body, often referred to as the "soma" or "perikaryon," and the cell processes, most notably the axon, make up a neuron. It is important to keep this in mind since it contributes to our understanding of pathogenetic pathways. The whole cell is a structure that contributes to the generation, conduction, and transmission of impulses (Cantile *et al*., 2015).

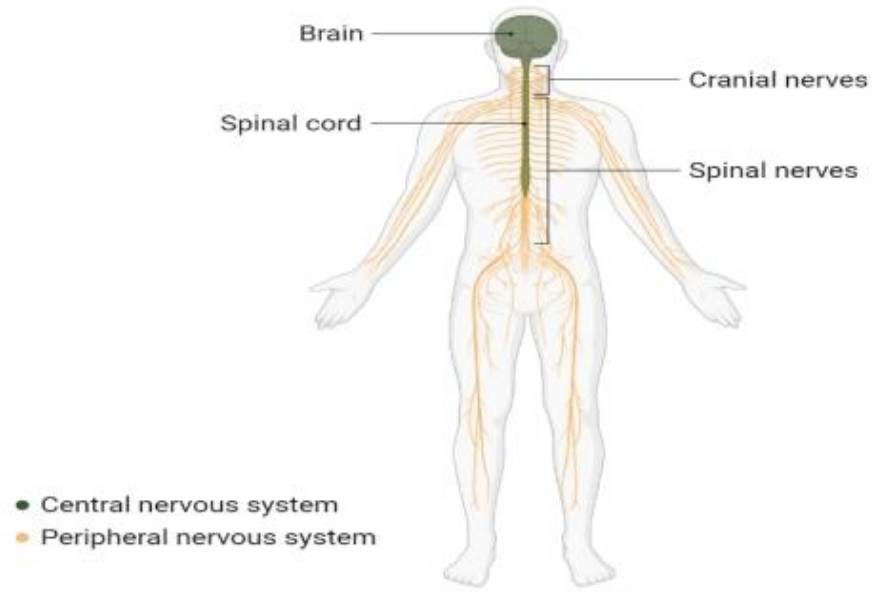

Figure 2.1 : Component of Nervous System (Created from https://app.biorender.com)

2.2 Alzheimer's Disease

Alzheimer's disease is a progressive, degenerative disorder that affects the brain and results in impaired memory, thinking, and behavior. It is the most common form of dementia, a heavy burden on health and socioeconomic elements in aging societies.

Worldwide, around 50 million people have Alzheimer's (AD) (BrightFocus Foundation). Two types of Alzheimer's disease are **early-onset Alzheimer's** disease and **late-onset Alzheimer's** disease. The critical distinction between the two is whether they begin before or after age. 65.5-8% of people over 65 and up to 50% of people over 85 are diagnosed with AD, showing a complex late-onset genetic inheritance (Kamboh, 2018). As a complex genetic condition, late-onset AD is thought to be 60 to 80 percent heritable (Rabinovici, 2019).

The AD process also results in various cognitive dysfunctions along with memory loss. Researchers investigated the relationship between Alzheimer's disease-related pathologic changes in frontal cortical brain biopsy and AD biomarkers in ventricular vs. lumbar CSF, as well as the relationship between AD biomarkers in CSF and cortical

biopsy and the final clinical diagnosis of AD (Seppälä *et al*., 2012) The buildup of amyloid plaques, neurofibrillary tangles in the brain, and cerebral atrophy is most frequently seen in the temporal area. Also, other neurodegenerative and cerebrovascular disorders might affect AD's clinical findings. (Knopman *et al*., 2021).

Mendelian or complex diseases can be due to mutational changes in DNA (Amberger *et al*., 2011). While environmental factors, such as lifestyle and diet, may play a role, AD also has a genetic component, with several alleles in specific genes increasing the risk of developing the disease. According to genetic classification, there are two main types of Alzheimer's disease: a sporadic form that is thought to be caused by a combination of genetic susceptibility and environmental exposures and a form that is inherited through autosomal dominant inheritance. It is difficult to estimate the exact prevalence of these two forms of the disease, as a wide range of factors can cause them, and the prevalence of the disease varies widely depending on age, genetics, and other risk factors (Cuyvers & Sleegers, 2016). Although it is uncertain how to use molecular pathways to diagnose Alzheimer's disease, several factors are thought to contribute to the illness's etiology (Moradifard *et al*., 2018).

Apolipoproteins (APO) are proteins that help transport cholesterol and other fats in the body. They are found in the outer coatings of lipoproteins, molecules that carry cholesterol and other fats through the bloodstream. Several apolipoproteins, including APOE, APOA1, and APOA2, play different roles in the metabolism of cholesterol and other fats. Dysregulation of apolipoprotein levels has been linked to an increased risk of cardiovascular disease and other health conditions. The protein apolipoprotein E (APOE) genotype is the most significant genetic risk factor for late-onset AD. The primary cholesterol transporter in the brain is encoded by the gene APOE (Rabinovici, 2019).

Amyloid precursor protein (APP) is a protein found in the brain and plays a role in the development and function of the nervous system. Research suggests that APP may be involved in the regulation of nerve cell function and communication, as well as the formation of new blood vessels in the brain. Genetic mutations in the APP gene have been linked to an increased risk of AD, but it is unclear how these mutations lead to the development of the disease. In people with Alzheimer's disease (AD), APP is

believed to be involved in forming amyloid plaques and abnormal protein deposits in the brain. These plaques are a characteristic feature of AD and are thought to contribute to the death of brain cells and the deterioration of brain tissue.

Astrocytes are the most prevalent cell type within the Central Nervous System (CNS). They are crucial for preserving brain homeostasis and protecting neurons. In both healthy and diseased conditions, astrocytes play crucial roles in synaptogenesis, the release of neurotransmitters, cognition, neuroinflammation, glycogen storage, the formation of the Blood-Brain Barrier (BBB), the clearance of toxic substances like glutamate excess, and K^+ spatial buffering, and the release of trophic factors for neurons and the other four brain cells (Hamby & Sofroniew, 2010 ; Posada-Duque *et al*., 2014). Astrocytes form a tripartite synapse with presynaptic and postsynaptic neurons based on their close morphological and chemical connections to the neurons through their processes (Perez-Alvarez & Araque, 2013) . They support and protect neurons and play various roles in the functioning of the nervous system. Astrocytes have been shown to be involved in regulating apoptosis and debris clearance following cell death. According to several studies, neurodegenerative illnesses like Alzheimer's Disease (AD) are characterized by astrocyte metabolic dysregulation (Parpura *et al*., 2011) .

2.3 SPOCK1

The SPOCK1 protein is a member of the SPARC (osteonectin) proteoglycan family. SPARC/osteonectin, cwcv, and kazal-like domains proteoglycan 1 (SPOCK1) is a glycoprotein isolated from human testes that initially belonged to the secreted protein, acidic, cysteine-rich (SPARC) family and was previously known as "testican-1". SPOCK1 is abundant in the brain, cartilage, vascular endothelium, myoblasts, fibroblasts, lymphocytes, and neuromuscular junctions (NMJs), highlighting that the proteoglycan plays a role in a variety of physiological functions and essential roles in the central nervous system diseases (Wang *et al*., 2017).

Recently in a 2016 study, expression level analysis revealed increased levels of Testican-1 in the frontal and temporal cortex of Alzheimer's patients; histological analysis revealed that Testican-1 accumulates and co-aggregates with A plaques in the frontal, temporal, and entorhinal cortices of Alzheimer's disease patients (Barrera-Ocampo *et al*., 2016). Proteomic analysis revealed ten fragments of Testican-1 in cerebrospinal fluid (CSF) from Alzheimer's patients. It suggested that it may modulate the endocytic pathway and lead to the accumulation of Aβ40 and Aβ42.

Moreover, "MPAIAVLAAAAAAAAWCFLQVES," consisting of the first 21 amino acids of SPOCK1 signal peptide, was identified as one of the body fluid markers of Alzheimer's disease in 2019 and has been patented. Studies done so far with SPOCK1 being extracellular in tumor tissues showed that it plays a role in regulating the matrix (ECM). SPOCK1 has been associated with 36 different tumors in studies, but SPOCK1 physiological functions are not yet clearly known.

Moreover, according to Rafatova (2022), we have identified two variants in the SPOCK1 gene region associated with (LOAD), supported by a case/control study.

2.3.1 Gene Structure of SPOCK1

The gene coding for it is located at 5q31.2, which means the long (q) arm of chromosome 5 at position 31.2 in humans. Gene starts at 136,310,987 bp and ends at 136,834,068 bp. Homo sapiens SPOCK1 gene accession number for RefSeq (mRNA) transcript in the NCBI database is NM_004598.4. It is a protein-coding gene with a coding sequence length of 519,905 bp. It spans at least 70 kb and comprises 11 exons (Sun *et al*., 2020). According to Ensembl, SPOCK1 has 11 transcripts (splice variants), 288 orthologues, and three paralogues. Sixteen phenotypes are associated with SPOCK1.

There are 11 transcripts listed in Ensembl;

1.SPOCK1-202(ENST00000394945.6) is 4824 bp in size and has 439 aa.

2.SPOCK1-201 (ENST00000282223.11) is 4488 bp in size and has 377 aa.

3.SPOCK1-209 (ENST00000510689.5) is 571 bp in size and has 67 aa.

4. SPOCK1-204 (ENST00000505690.1) is 453 bp in size and has 139 aa.

5.SPOCK1-211 (ENST00000635347.1) is 648 bp in size and has no protein.

6. SPOCK1-207 (ENST00000509978.1) is 572 bp in size and has no protein.

7. SPOCK1-206 (ENST00000509293.1) is 553 bp in size and has no protein.

8. SPOCK1-205 (ENST00000508642.1) is 499 bp in size and has no protein.

9. SPOCK1-203 (ENST00000503916.1) is 480 bp in size and has no protein.

10. SPOCK1-208 (ENST00000510405.5) is 399 bp in size and has no protein.

11. SPOCK1-210 (ENST00000515091.1is 560 bp in size and has no protein.

SPOCK1 has 11 exons in total. Exons 2, 3, 4, and 8 overlap to form the first, second, and fourth osteonectin domains. Exons 5 and 6 code the third osteonectin and Kazal-like domains. Exon 10 encodes the CWCV domain. The exons nine and 10.2-containing residues 310 and 379, which comprise the Thyropin domain, are related.

2.3.2 SPOCK1 Protein

Hevin(SC1), the modular calcium-binding protein 1 and 2, and the follistatin-like protein 1 are all members of the SPARC family, including SPARC, SPOCK1, SPOCK2, and SPOCK3. Each member of the SPARC family has a basic structure that consists of an N-terminus, a follistatin-like domain, and a C-terminus. SPOCK1 carries both heparan and chondroitin sulfate chains, SPOCK2 is N-glycosylated, and SPOCK3 is made up of multiple mucin-type O-glycans indicating that each SPOCK has a different physiological function. In contrast, SPOCK2 and SPOCK3 are pure heparan sulfate proteoglycans. SPOCK1 gene, located on chromosome 5q31, encodes the 439 amino acids that make up the SPOCK1 protein. The SPOCK1 gene encodes the protein core of a seminal plasma proteoglycan containing chondroitin and heparan-sulfate chains.

The SPOCK1 gene encodes the testican-1 protein. Multidomain protein SPOCK1 has homologies to several protease inhibitors. The proteoglycan has an N-terminus, a follistatin-like domain, an extracellular calcium-binding domain, a thyropin domain, a

domain V, two possible glycosaminoglycan attachment (GAG) sites, and a C-terminus (Figure 2.2).

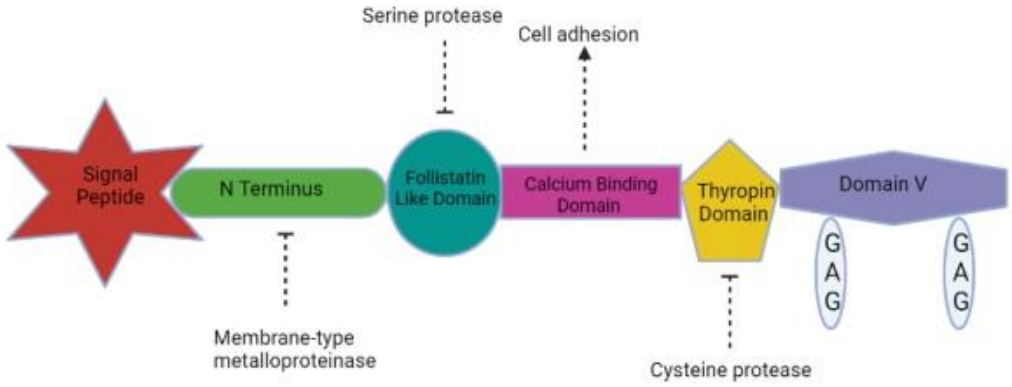

Figure 2.2 : Structure of SPOCK1 (Created from https://app.biorender.com based on Bocock *et al*.,2013)

The compound's N-terminus inhibits an unusual membrane-type metalloproteinase. The six-cysteine-follistatin-like domain and the Kazal domains in serine protease inhibitors share similarities. The extracellular calcium-binding domain, a separate domain member of the SPARC family, facilitates cell adhesion. The 64 amino acids that make up the thyropin domain are homologous to protein sequences that block cysteine proteases.

Cathepsin-L. SPOCK1 is a highly conservative chimeric proteoglycan that carries both heparan sulfate and chondroitin sulfate chains and can be categorized as belonging to a subset of the osteonectin domains. SPOCK1 is categorized as a cell surface-interacting ECM regulator because of its modular structure (Sun *et al*., 2020).

SPOCK1 protein functions as the core of a seminal plasma proteoglycan modified post-translationally to include chondroitin and heparan-sulfate chains. The molecular functions include binding calcium ions and inhibiting serine-type endopeptidases, metalloendopeptidases, and cysteine-type endopeptidases. It is involved in various biological processes, including cell adhesion, differentiation of central nervous system neurons, inhibition of cell-substrate adhesion, endopeptidase activity, the growth control of cells, and the development of the nervous system.

The figure below shows the interactions between the 25 gene products that possibly interact with the testican-1 protein (Figure 2.3).

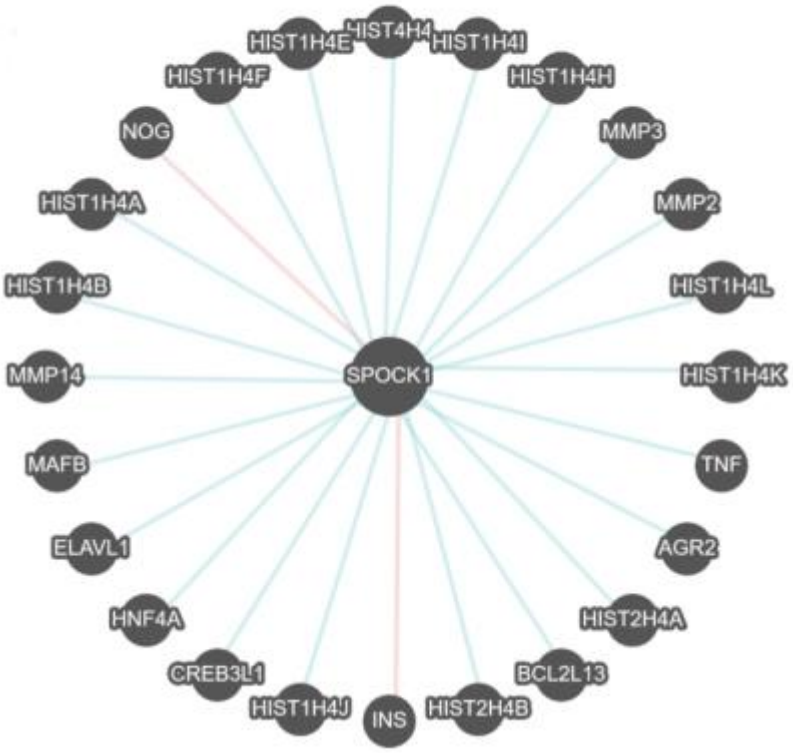

Figure 2.3 : Interaction between SPOCK1 and 25 other gene products. (Created from https://genome.ucsc.edu/cgi-bin/hgGeneGraph)

According to the 2020 study's results, the relationship between astrocytes and microglia cells via APOE is one of the significant contributors to Alzheimer's (Figure 2.4). Aβ in the intercellular fluid is a stimulating signal for astrocytes. Intercellular binding of APOE is released from astrocytes to LRP1 in the microglia membrane by forming a complex with Aβ. It has a role in the clearance of Aβ deposits fluid by being taken into the cell by microglia. In addition, Aβ has the potential to activate astrocytes directly via α7-nAchR, CaSR, CD36, CD47, and AQP4. Active damage to neurons via astrocytes, extracellular glutamate dyshomeostasis/excitotoxicity, TNF-α, IL-1β, and IL-6 can give (Guo *et al.*, 2020). One speculation on SPOCK1's role is to contribute

to the effect of APOE on cleaving extracellular Aβ plaques as an extracellular matrix regulator.

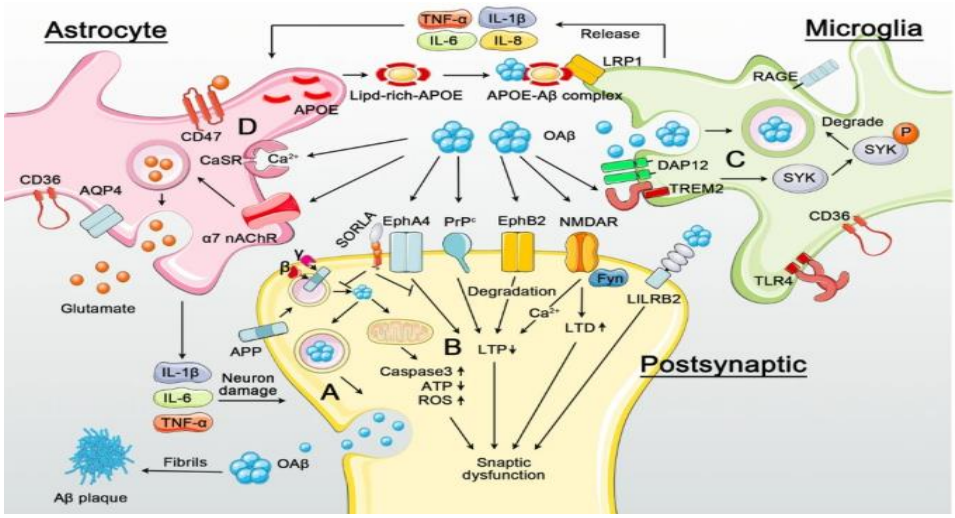

Figure 2.4 : Postsynaptic regulation in regards to AD (Taken from Guo *et al*., 2020)

2.4 Astrocyte

Numerous mechanisms connected to brain function and the development of disease include astrocytes. In addition to neurotransmitters (and their precursors), modulators, peptides, hormones, trophic (growth) factors, and metabolites, astrocytes are important secretory cells. The development, function, and plasticity of synapses, the growth, differentiation, and survival of neurons, as well as the control of vascular tone and blood flow in the brain, have all been linked to astrocytic-released substances (Chung *et al*., 2015, Verkhratsky *et al*., 2016). Astrocytes are a group of cells that vary in their morphology and functional properties depending on where in the brain they are found. After birth, astrocyte progenitors go to the brain and its associated regions. They regulate blood-brain barrier permeability control, extracellular homeostasis maintenance, and brain processes associated with neurogenesis and synaptogenesis. A mature astrocyte's expression of some more prevalent genes in cell progenitors suggests that it still has some proliferation potential (De Zeeuw and Hoogland, 2015). It is not surprising that problems in these cells are linked to a wide variety of various neuro-pathologies, given the variability of the cell population. The astrocytes' active

inflammatory state, typically described as the up-regulation of glial fibrillary acidic protein, is a hallmark of brain disorders (GFAP). In particular, the aging brain and neurodegenerative diseases like Alzheimer's and Huntington's disease may be affected by the decreased astrocyte activity brought on by cellular senescence. Due to their Ca^{2+} signals and the fact that it is closely associated with the illness severity/condition, astrocytes can also promote the initiation and development of the inflammatory state (Peteri *et al*., 2019). They also play a role in the aberrant neuronal activity seen in several disorders of the frontal cortex, including ischemic stroke and epilepsy. In a recent study, the state of understanding astrocytes' role in brain diseases discussed the potential for using them as a target for therapy for neuropathologies (Siracusa *et al*., 2019).

2.5 Neuroblasts

A postmitotic cell that does not divide further and eventually grows into a neuron in vertebrates is called a neuroblast or primitive nerve cell (Sadler *et al*., 2010). Neuroblasts are neural progenitor cells that divide asymmetrically to produce a neuroblast and a daughter cell of different potency depending on the type of neuroblast in invertebrates like Drosophila. Radial glial cells differentiate into vertebrate neuroblasts and are dedicated to producing neurons (Williams *et al*., 2001). Radial glial cells develop gradually from neural stem cells, which can only divide symmetrically to make more neural stem cells (Purves *et al*., 2012). Radial glial cells, also known as radial glial progenitor cells, undergo asymmetric division to give rise to a neuroblast and a second radial glial cell that will re-enter the cell cycle (Johnson *et al*., 2017).

When a radial glial cell splits to become the neuroblast, it does this by mitosis in the germinal neuroepithelium (also known as the germinal zone). While the radial glial progenitor cell produced by the neuroblast remains in the lumenal epithelium, the neuroblast separates from the epithelium and migrates. The migrating cells' ability to differentiate into neurons will depend on the places they occupy (Rossi & Volterra, 2012).

2.6 Mitochondria

Mitochondria are essential for many cellular processes, including ATP production, intracellular Ca^{2+} signaling, and reactive oxygen species generation. Neurons rely heavily on a mitochondrial function to establish membrane excitability and carry out complex neurotransmission and plasticity processes.

The most common kind of dementia in elderly people is Alzheimer's disease, which is characterized by extracellular amyloid plaques and intracellular neurofibrillary tangles in AD patients' brains. Numerous indicators point to the amyloid-beta (A) protein, which is produced from its precursor protein APP, as being essential to the development of AD. Additionally, it has been established that the early AD events were impairments in energy metabolism and mitochondrial malfunction (Rhein *et al*., 2009). While studies on isolated mitochondria and dissociated cell cultures have yielded a wealth of information, little is known about mitochondrial function in intact neurons in brain tissue (Thevenet *et al*., 2016). However, understanding the complex physiological behavior of neurons, as well as the pathophysiology of various neurological diseases, requires a detailed description of the interactions between mitochondrial function, energy metabolism, and neuronal activity (Kann & Kovács, 2008). Amyloid peptide, a key component in the pathogenesis of Alzheimer's disease, has been shown to impair mitochondrial function. Amyloid beta plaques can interact with mitochondria and cause mitochondrial dysfunction. One of the most widely accepted hypotheses for the onset of Alzheimer's disease proposes that mitochondrial dysfunction and oxidative stress are primary events in the pathology's emergence (Picone *et al*., 2014).

CHAPTER 3

MATERIALS & METHODS

3.1 Materials

The materials can be listed as cell culture of SVG p12 and SH-SY5Y cell lines, the antibody of SPOCK1, and Tagged constructs.

3.1.1 Mammalian Cell Culture

Two different cell lines were cultured during this study. SH-SY5Y is a neuroblastoma cell line, and SVG p12 is an astrocyte cell line selected for conducting experiments.

3.1.2 Human Neuroblastoma Cell Line (SH-SY5Y)

The neuroblastoma cell line SK-N-SH was the source of the triple-subcloned cell line SH-SY5Y. The cells can be transformed into various functioning neurons by adding particular substances, so it acts as a model for neurodegenerative diseases. The SH-SY5Y cell line has also been extensively employed in experimental neurological research of the nervous system, including examinations of neuronal metabolism, differentiation, and function of neurodegenerative, neurotoxic, and neuroprotective processes.

In this study, to visualize and investigate the intracellular location of the SPOCK1 gene product, the SH-SY5Y cell line was used. This cell line's cultivation and proliferation process can be maintained and completed in 4 to 7 days. The percentage of transfection is relatively low. This cell line was ordered from the ATCC Company, England.

3.1.3 Human Astroglia Cell Line (SVG p12)

By transfecting cultured human fetal glial cells from brain tissue removed from 8–12 week-old embryos with DNA from an ori–mutant of SV40, the SVG p12 cell line was created. They have adherent growth features, and the cultivation and proliferation process can be maintained and completed in 2-3 days. This cell line was also ordered from the ATCC Company, England.

3.1.4 Cell Media

In this study, four different cell media were used:

The first one is Eagle's Minimum Essential Medium which is suggested for the SVG p12 cell line. The medium was prepared by mixing EMEM (Biological Industries Cat Number 01-025-1A), 10% FBS(Biological Industries Catalog Number 04-001-1A), and 1% Penicillin/Streptomycin (Biological Industries Catalog Number 03-031-5B).

The second one is EMEM: F12 Medium which is suggested for the SH-SY5Y cell line. The medium was prepared 1:1 mixture ratio of Eagle's Minimum Essential Medium (Biological Industries Catalog Number 01-025-1A), F12 Medium (Biological Industries Catalog Number 01-095-1A), 10% FBS (Biological Industries Catalog Number 04-001-1A), and 1% Penicillin/Streptomycin (Biological Industries Catalog Number 03-031-5B).

The third one is OPTIMEM media which was used for the transfection of cells, and it contains HEPES and sodium bicarbonate buffer, with hypoxanthine, thymidine, sodium pyruvate, L-glutamine or GLUTAMAX, trace elements, and growth factors added.

The last one was used to cultivate the SVG p12 cell line. After a few passages and proliferation, the SVG p12 cell line medium changed with DMEM (Gibco Catalog Number 11965092) medium to maximize and accelerate the growth.

3.1.5 Maintenance

The maintenance of both cell cultures required an incubator that can be used at 5% CO_2 and 37ºC. The laminar flow cabinet (Nuve LN 120) was used for medium change, passage, and transfection. For SH-SY5Y every seven days and SVG p12 every five days, the passage of the cell was performed after reaching confluency. Firstly, the cells were washed with PBS, and then Trypl-E Express with phenol red (Gibco Cat Number 12605-028) was added to remove them from the attached surface. T25 and T75 flasks were used for the cultivation of both cell lines. The formulation of PBS is given in Appendix A.

3.1.6 Other Chemicals and Materials

The transfection procedure was performed by using Lipofectamine LTX Plus (Invitrogen Catalog number 15338-100) and Lipofectamine 2000 (Invitrogen Catalog Number 11668019), purchased from Invitrogen (MA, USA). The protocol of this process is given below.

3.1.7 The Strain of Bacteria and Bacterial Growth Media

Escherichia coli XL1-Blue was used in experiments involving the bacterial transformation. Luria Bertani solution was made and autoclave sterilized for 20 minutes at 121 ºC using a Nuve OT 40L autoclave machine as bacterial growth culture media. Ampicillin (100 g/ml) was employed to apply bacterial selection using antibiotics. Bacterial colonies that had transformed were obtained from LB agar plates that had been incubated in Zhicheng Instruments' ZHWY-200B incubation apparatus for 16 hours at 37 ºC. The collected colony inoculation was cultured using liquid LB solution and inoculated in the Zhicheng Instruments ZHWY-200B rotary shaker at 200 rpm for 16 hours at 37 ºC.

3.1.8 Plasmid, Primers, and Sequencing

The tagging experiments were designed for the C-terminus and 31st position of SPOCK1 with EGFP or mCherry constructs. The detailed primer designs can be seen in Appendix B.

3.1.9 Other Chemicals and Materials

The remaining necessary chemicals for the project were purchased from Sigma Chemical Company (NY, USA).

Thermo Scientific (MA, USA) sells molecular cloning enzymes such as Phire Green Master Mix DNA polymerase, T4 ligase, and 6X DNA dye, and New England Biolabs sells restriction enzymes (MA, USA). We bought Generuler from Fermentas. Kits for extracting plasmids from gel and miniprep were purchased from Thermo Scientific.

3.2 Methods

3.2.1 Cloning

In this study, we used the pBlueScriptR Plasmid (Clone number 4821322) from DNAclone, ordered from Japan, containing the SPOCK1 gene. The vector type is phagemid, and it is ampicillin resistant. The gene of interest is located between XhoI, and BamHI cut sites. Also, it has a polylinker sequence shown below: GAATTCGTCGACTCGAGCGGGGATCCGGCCATAAGGGCCTGATCCGTCGAGGGGGGG CCCGGTACC

3.2.2 Preparation of Competent *E.coli* Cells by Rubidium Chloride Method

To prepare competent *E.coli* XL1-Blue cells, first, the cells were streaked on an antibiotic-free LB agar plate and incubated for 16 hours at 37 °C. After incubation, a

single colony was picked and inoculated with 2 ml of antibiotic-free LB media. The inoculated growth tube was incubated in a shaker for 16 hours.

At 37 °C, 200 rpm, the culture was inoculated overnight in an antibiotic-free LB culture medium containing 20 mM MgSO4 in a 1:100 (v:v) ratio. The inoculated flask was incubated in a shaker at 37ºC, 200 rpm, until the optical density reached 0.4-0.6. When subcultures reach an OD of 0.4-0.6 at 600 nm, isolate cultures, place them in 50 ml falcons, and centrifuge at 4000 rpm for 5 min at 4 ºC.

During centrifugation, the supernatant was discarded, and the pellet was gently dissolved in 20 ml of TFB1 solution and incubated on ice for 5 min. Afterward, the pellet dissolved in TFB1 solution and was centrifuged at 2000 rpm for 5 min at 4 ºC.

3.2.3 Polymerase Chain Reaction (PCR)

Plasmids containing SPOCK1, EGFP, and mCherry were amplified via PCR for further experiments. Primers to remove the stop codon from SPOCK1 were designed to generate C-terminus tagging. The detailed primer designs can be seen in Appendix B.

Table A: Optimal PCR Component for SPOCK1 Tagging

Reagent	**Amount**
DNA template	250-300 ng
Forward Primer	1.25 µl
Reverse Primer	1.25 µl
Phire Green MM	25 µl
NFW	Up to 50 µl

Table B: Optimal PCR Condition for SPOCK1 Tagging

Step	Temperature	Time	
Pre-denaturation	98 ºC	0:30 s	
Denaturation	98 ºC	0:05 s	33 cycles
Annealing	69 ºC	0:05 s	
Extension	72 ºC	1:00 min	
Final Extension	72 ºC	1:00 min	

3.2.4 Insertional PCR Method

Fluorescent protein genes with the appropriate overhang regions were amplified using PCR. For the second PCR reaction, the products of the first PCR (mega primers) were used with a 1:5 template: primer ratio. The matched regions of the mega primer bind to the SPOCK1 gene matching region (around the 31st position), creating a new artificially produced non-methylated plasmid. All methylated unlabeled template plasmids were digested using DpnI. If DpnI digestion does not cut all parental plasmids, the bacteria will take up these non-EGFP/mCherry-inserted parental plasmids (which contain the ampicillin resistance gene). As a result, some colonies on our ampicillin agar plates will be false positives, indicating that they do not contain the desired plasmid. The conditions of the method and a schematic figure about the method are given in Table C and D and Figures 3.1 & 3.2.

Table C: Optimal PCR Protocol Component

Reagent	Amount
DNA template (Spock1 containing pBlue Script)	25 ng
Mega primer	125 ng
5x Buffer	10 µl
dNTP mix (10 mm)	1.25 µl
Phusion HS II Master Mix	1 µl
Nuclease Free Water	Up to 50 µl

Table D: Optimal condition for Insertional PCR Protocol

Step	Temperature	Time	
Pre-denaturation	98 ºC	3:00 min	
Denaturation	98 ºC	0:30 s	18 cycles
Annealing	57 ºC	0:45 s	
Extension	69 ºC	10:00 min	
Final Extension	69 ºC	12:00 min	

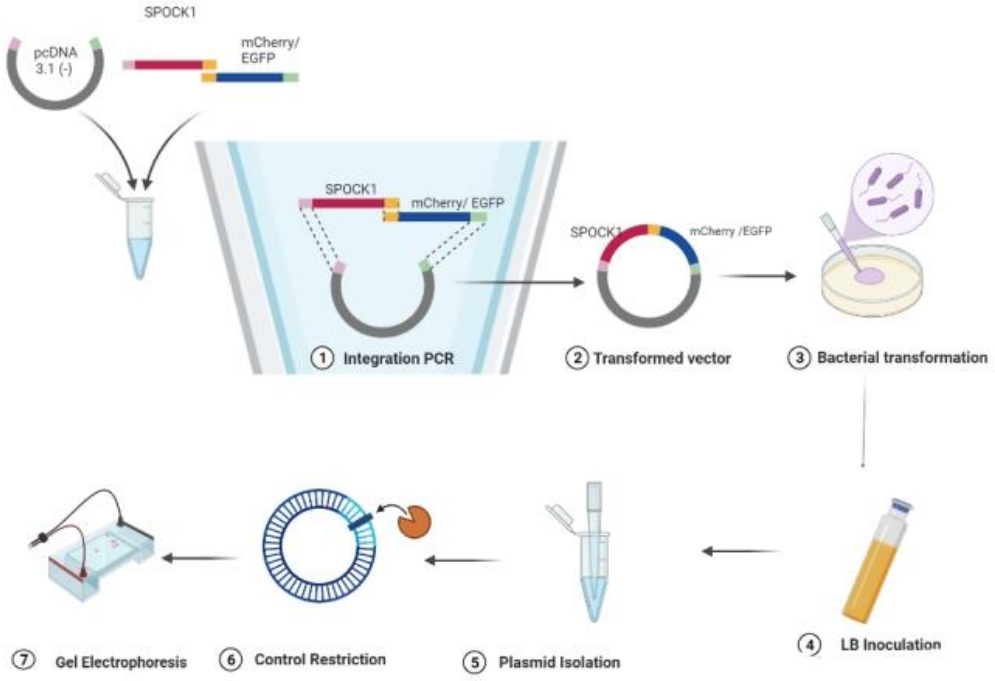

Figure 3.1 : Representation of C-Terminus Tagging Protocol (Created from https://app.biorender.com)

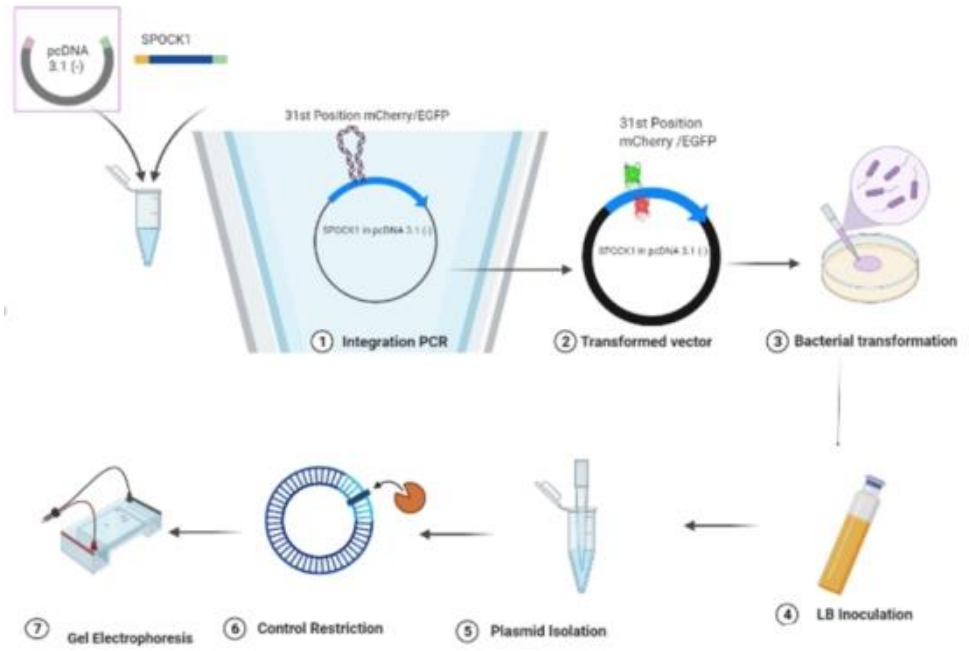

Figure 3.2 : Representation of 31st Position Tagging Protocol (Created from https://app.biorender.com)

3.2.5 Agarose Gel Electrophoresis

Using a 1% agarose gel, PCR-amplified DNA samples and restriction products for fluorescent protein tagging were seen to control and validate amplification. On the other hand, 2% agarose gel was used to visualize DNA samples for minigene production. The 100 ml agarose gels were produced, and 22 µl of Ethidium Bromide (EtBr) was added as a DNA chelator for UV-light visualization. First, 60 ml of 1X TAE buffer was added along with 0.64 g or 1 g of weighted agarose for a 1% or 2% gel. The mixture was microwaved until the agarose crystals were completely dissolved. After cooling the liquid agarose gel mixture with tap water for 30 seconds, 22 µl of EtBr was added and thoroughly mixed. The gel was added to a gel box that had the proper combs. DNA samples were generated by diluting loading dye (Thermo Scientific, Catalog Number 0611) from 6X to 1X after polymerization. The samples were put into wells, and a DNA marker called Generuler (Fisher, Catalog Number 11803983) was loaded. With 110V, the samples were run for 50 minutes. The

preparation of a 50X TAE buffer stock solution detailed protocol is provided in Appendix A.

3.2.6 Extraction from Agarose Gel

Loading PCR and restriction product amplification onto agarose gel allowed UV visualization. DNA bands were cut and put into 1.5 ml microcentrifuge tubes after being compared to the DNA ladder's proper location. Microcentrifuge tubes containing gel were weighed, and the weight of the empty tubes was deducted. According to the kit's instructions, DNA was extracted from the agarose gel using the GeneJET Gel Extraction Kit (Thermo Fisher Scientific, Catalog Number K0691). To improve the yield of eluted DNA, 30 µl of warmed, nuclease-free water rather than the kit's recommended 30 µl of elution buffer was used for DNA elution from the column membrane in the last step.

3.2.7 DNA Concentration Measurement

The BioDrop LITE instrument was used to measure the yield of DNA products. We rinsed the sample loading area with distilled water before measurement to clean the remaining samples from previous measurements. Then the device opened and self-calibrated. 1 µl of nuclease-free water was used as the blank, and the option of the "Life Sciences" section and DNA subsection were chosen. 1µl of DNA was placed onto the sample loading space after the blank measurement, and the measurement was taken.

3.2.8 Restriction Enzyme Digestion

Restriction enzymes were purchased from New England Biolabs Inc. (NEB) (MA, USA) for this study. After the procedure of restriction, sticky-end constructs were produced. The restriction process was carried out as recommended by NEB's instruction manual, using 1 unit of enzyme for 1mg of DNA. In this work, 1 µl of enzyme and 1.5 µl of CutSmart NEB buffer were utilized for the restriction operations,

and the total volume was completed to 20 µl. The finished mixture was incubated at 37 ºC for 1.5 hours.

3.2.9 PCR Purification

It was carried out using the Thermo Scientific GeneJet Purification kit (Catalog Number K0702) to eliminate restriction components and purify the DNA product. The kit's instructions were followed, and to boost the yield, the elution step was carried out using 30 µl of nuclease-free water rather than 50 µl EB.

3.2.10 Ligation

The constrained compatible DNA products and the vector plasmid were covalently bound using a ligation process. Sticky-end restriction products were inserted into this study's expression vector pcDNA3.1 (-) using the ligation technique. Based on the 150 ng vector, ligation ratios of 1:5 and 1:10 were computed. At least 150 ng of a limited vector, an insert, 1 µl of T4 DNA ligase enzyme (NEB, Catalog Number 0202T), 2 µl of 10X T4 DNA ligase buffer, and 20 µl of nuclease-free water make up the ligation reaction. The ligation reaction was incubated for 16 hours at room temperature.

3.2.11 Transformation of Competent *E.coli* Cells

A vector carrying the desired gene was introduced into a bacterial host according to a technique for bacterial transformation. This procedure was used in this investigation for amplifying plasmids and ligation products. To achieve competency, *E. coli* XL1 blue, treated with RbCl, was utilized as the bacterial host and kept at -80 ºC. Competent cells were removed from -80 ºC and placed on ice for 15 minutes. 50 µl circular plasmid and 3 µl of ~150 µl/ng ofligation product were put into a competent cell tube under sterile conditions after 15 minutes of incubation. For 30 minutes, the DNA and bacterial mixture were incubated on ice. The tube containing the DNA and the competent cells was subjected to a heat shock at 42 ºC for 45 seconds. After that, the tube was incubated for 5 minutes on ice. After incubation, 250 µl LB was added to the

tube and shaken at 37 ºC at 180 rpm for one hour. Following a 4000 rpm centrifugation, 200 µl of the supernatant was removed from the tube, and the pellet was dissolved in the remaining LB. Given that pcDNA3.1(-), contains an ampicillin resistance gene, the dissolved pellet was spread on LB agar plates that had been prepared with ampicillin.

For bacterial colony growth, agar plates were incubated at 37 ºC for 16 hours.

3.2.12 Plasmid Isolation from *E.coli*

The GeneJET plasmid miniprep kit (Catalog Number K0503) from Thermo Scientific was used for plasmid DNA isolation. A single colony was chosen from the agar plate and inoculated into 5 ml of LB with 5 µl of 1000X ampicillin under sterile conditions. A bacteria colony and LB with antibiotics were cultured for 16 hours at 37 ºC at 180 rpm. After incubation, the LB tube was centrifuged at 4000 rpm. After the supernatant was discarded, the kit's protocol was applied to the pellet. The elution step was carried out to enhance yield using 100 µl nuclease-free water rather than 100 µl EB.

3.2.13 Passage and Cell Seeding

Mammalian cell lines SH-SY5Y and SVG p12 were ordered from the ATCC Company, England. The neuroblastoma cell line, SH-SY5Y, can divide in approximately 48 h; the passage was done after 3-4 days of incubation. The other cell line is the SVG p12, astrocytes have adherent growth features, and the cultivation and proliferation process can be maintained and completed in 2-3 days.

The cell lines were expanded onto a T25 flask and incubated there for the incubation period at 37 ºC and 5% CO_2. The flasks were placed in a laminar flow during the passage process, the cell media inside the flask was removed, and cells were gently washed with warm 3 µl 1X PBS diluted 10X PBS. PBS was then removed, and 500 µl of Trypl-E was added to the cells. The flask was put into a 37 °C incubator with 5 % CO_2 and left there for 5 minutes. After that, 4 ml of recommended media was gently pipetted into the incubated flask in the laminar flow. 6ml of recommended media were put into a new T25 flask that had been labeled. The old flask's 200 µl cell medium containing SH-SY5Y and SVG p12 cells was transferred into the newly labeled flask.

Up to the subsequent passage, the new flask was cultured at 37 ^{o}C in a 5% CO_2 incubator.

10 µl of the cell solution was transferred onto the hemocytometer for counting. The cells at four squares were counted under a microscope at 100X magnification , and the total number was divided by four and multiplied by 10.000 to get the number of cells in 1 ml suspension. We estimated and seeded 200.000 cells for 35mm plastic dishes and 35mm glass bottom dishes. Plastic bottom dishes were utilized for plate reader tests, and glass bottom dishes were used for microscope imaging.

3.2.14 Transfection of Mammalian Expression Vector and Organelle Markers to Cell Lines

The process of introducing nucleic acids into cells is known as transient transfection. Non-viral gene delivery is commonly referred to as transfection. Transfection of animal cells typically entails creating transient pores in the cellular membrane that allow genetic material to enter the cytoplasm. Transfection can cause morphologic and functional changes in target cells. Transfection of primary cortical and hippocampal neurons has proven to be a significant challenge in investigating neuronal gene functions. Many transfection methods have been developed over the last three decades, including electroporation, nucleofection, calcium phosphate co-precipitation, and lipofection. A lipid aggregate fuses with the negatively charged plasma membrane to deliver genetic material into cells. Cationic lipid molecules are frequently combined with neutral helper lipid molecules to increase fusion capacity. Lipofection reagents have been developed in a variety of formulations. Lipofection is a simple technique that is generally less toxic to cells. Although the technique achieves high transfection efficiencies in various cell types, transfection efficiency in postmitotic neurons varies (Sariyer, 2016).

A transfection approach was utilized to insert DNA samples into mammalian cells artificially. Since Lipofectamine LTX with Plus Reagent (Maurisse *et al*., 2010). from Invitrogen (MA, USA) has a transfection efficiency rate of more than 80%, transient transfection was carried out utilizing this product for this research The used organelle markers were kindly gifted from HHMI's Janelia Research Campus in Ashburn,

Virginia, USA. Organelle markers and fluorescently tagged SPOCK1 constructs were used in the transient transfection of the cell lines. On glass and plastic dishes, 150.000 and 200.000 cells were seeded for the transfection procedure, followed by adding 2 ml of medium. Before transfection, the plates were incubated for 24 hours to allow for cell adhesion. The next day, 100 µl of OptiMEM was combined with 300–500 ng of plasmid DNA for microscopy imaging. 100 µl of OptiMEM and 4 µl Plus reagent were added to tubes containing plasmids. At room temperature, the mixture was incubated for 15 minutes. A brand-new set of 100 µl OptiMEM tubes was made during incubation. Tubes with only OptiMEM were added 4 µl of Lipofectamine LTX. Following the incubation period, the tubes containing plasmid DNA and 100 µl of OptiMEM with additional lipofectamine were combined with the tubes containing PlusReagent and 100 µl of OptiMEM. The resultant combination was incubated at room temperature for 15 minutes. Dishes containing cells were removed from the incubator during incubation, and the media was suctioned out of the dishes. 1 ml of 1X PBS was used to wash the cells gently. After aspirating 1 ml of PBS, 680 µl of OptiMEM was added on top of the cells. After the incubation period, 200 µl of the transfection mixture was added to 680 µl of OptiMEM covering the cells. After 3 hours of incubation at 37 ºC and 5% CO_2, 2 ml of medium was added to the dishes. The dishes were imaged after two days of transfection using the confocal microscope. After imaging, cells were fixed using 4% PFA.

3.2.15 Immunohistochemistry

Immunohistochemistry studies were conducted with rabbit anti-SPOCK1 antibody (Goat anti-rabbit antibody, Alexa Flour 488 used as a secondary antibody to detect anti-SPOCK1 antibody). After fixing the cells with paraformaldehyde (4%) for 15 min at RT, they are rinsed three times with PBS. The samples were incubated in 0.2% Tween-20 for 15 min at 37 °C. After rinsing three times with PBS, the background was blocked with 1% BSA containing PBS (10 mM, pH 7.4) solution at 37°C for 15 min. The samples were incubated in the primary Ab (anti-Spock, 1:500 in 0.1% BSA) solution overnight at +4 °C. The cells were washed three times with PBS and incubated with the secondary Ab (Alexa Fluor 488 labeled, 1:5000 in PBS) for one h at 37 °C.

After rinsing three times with PBS, the samples were counterstained with DRAQ5 solution (diluted 1:1000 in PBS) for 30 min at RT. After a final three times wash with PBS, the cells were examined with confocal or fluorescence microscopes.

3.2.16 Confocal Imaging

Epifluorescence microscope is the most commonly applied microscope type used in biological sciences. A wide-field epi-fluorescence device and an electronic system are coupled to create a confocal microscope. This setup includes laser illuminators, a scanning head with electronic and optical components, a computer system for displaying and monitoring images, and the necessary software to adjust the signal, process the images, and analyze them.

The focal point of confocal imaging is the successive light collection. One method to capture an image with a Nipkow disc is to use the signal point by point. The technology can reduce non-focused light thanks to the Nipkow disc by rotating and revolving the tiny holes. Only concentrated light is therefore anticipated to reach, theoretically, the specimen. Consequently, the stage and beam remain stable, and the image obtained is clearer and more detailed. In Figure 3.3, a schematic explanation of confocal microscopy is given.

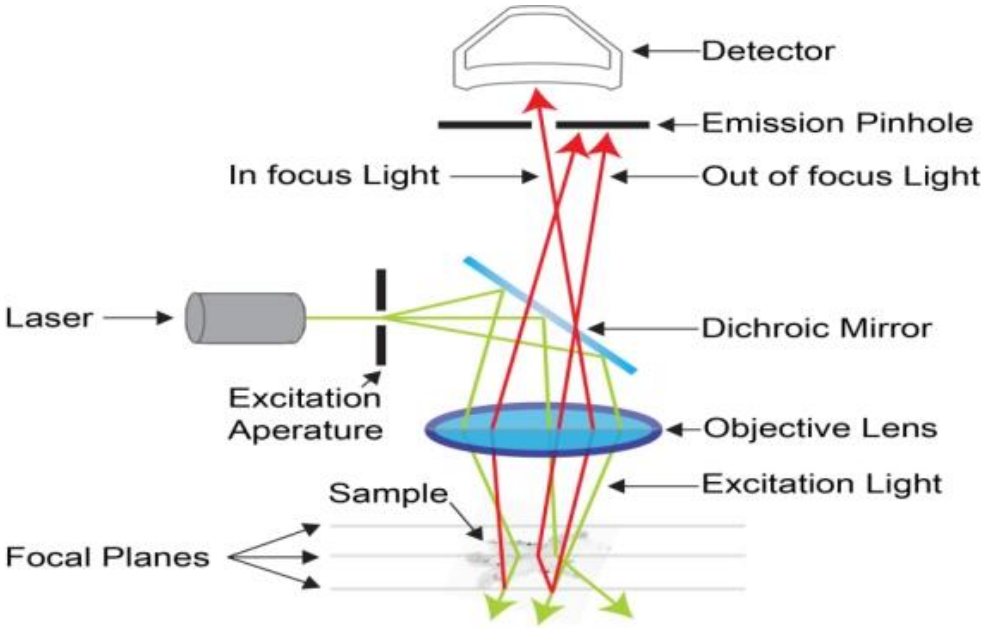

Figure 3.3 : Schematic explanation of Confocal Microscopy

SVG p12 and SH-SY5Y cells were transfected with EGFP and mCherry-tagged SPOCK1 proteins. Following incubation, glass-bottom dishes were imaged using Zeiss LSM 910 confocal microscope, and plastic dishes were imaged using Leica DMI 4000 with an Andor DSD2 spinning disc confocal microscope. The Andor DSD2 spinning disc microscope was used since it offers a maximum frame rate of 22 frames per second, a 410–750 nm emission range, and a 370–700 nm excitation range. Sharper images were produced, and non-focused light was rejected thanks to the spinning disc. A 63X immersion oil NA 1.4 objective lens was used for the imaging procedure.

The Zeiss Laser scanning microscope (LSM 910) was used since it offers a laser module with 405, 488, and 561 nm excitation range. C Epiplan APOCHROMAT objectives have been specially developed for confocal microscopy and provide minimal aberrations at 405 nm over the entire field of view. Images were taken with 63x immersion oil objective.

3.2.17 Bleed-Through

When acquiring a multi-channel image in a fluorescence microscope, crosstalk (crossover or bleedthrough) can occur. In that case, the emission radiation of a given emission wavelength is detected by the incorrect detector because some of the photons pass through the incorrect optical path inside the microscope (for example, because the spectral profiles of the fluorophores overlap and filters cannot separate the channels completely). As a result, some signals are recorded as coming from one dye when they actually come from another. To avoid this, microscopes typically excite each dye alternately, ensuring that all detected radiation comes from a single dye type (Gadella, 2008).

CHAPTER 4

RESULTS

4.1 Cell Culture

Two different cell lines were cultured for this study. Different morphological structures and growth patterns were observed as expected.

The protein expression and localization in these cells were investigated by tagging the SPOCK1 protein in neural cells (neuroblastoma and astroglia). Neuroblastoma and astroglia cells were cultured up to their 25th passage for different growth parameters, cell shapes, and localization of the SPOCK1 gene, which is thought to play an important role in Alzheimer's disease, were observed. Inverted light microscope images of the first passages taken with a Zeiss Primovert Microscope are below (Figures 4.1 & 4.2).

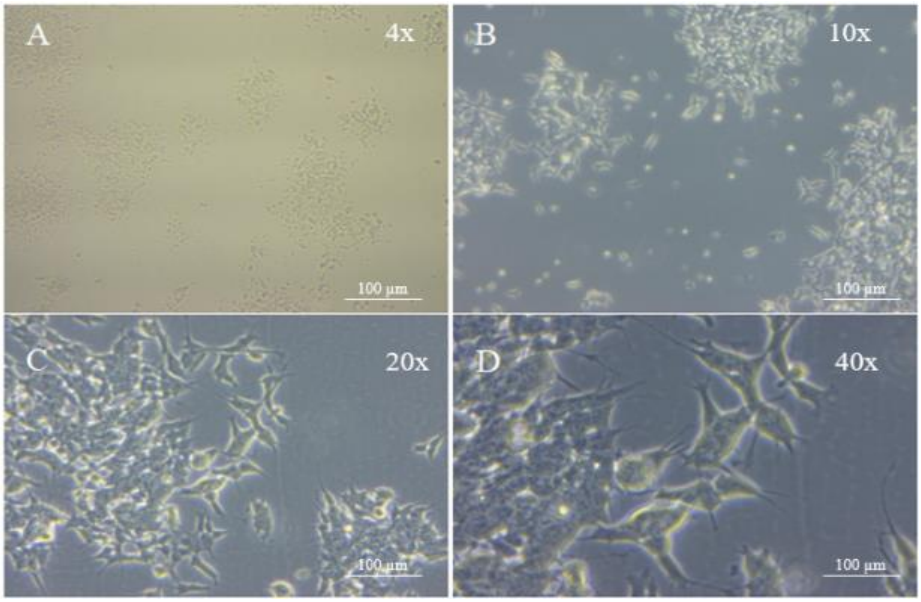

Figure 4.1 : SH-SY5Y Cell Line imaged with Zeiss Primovert Microscope in bright field mode A) with 4x B)10x C) 20x D) 40x magnification.

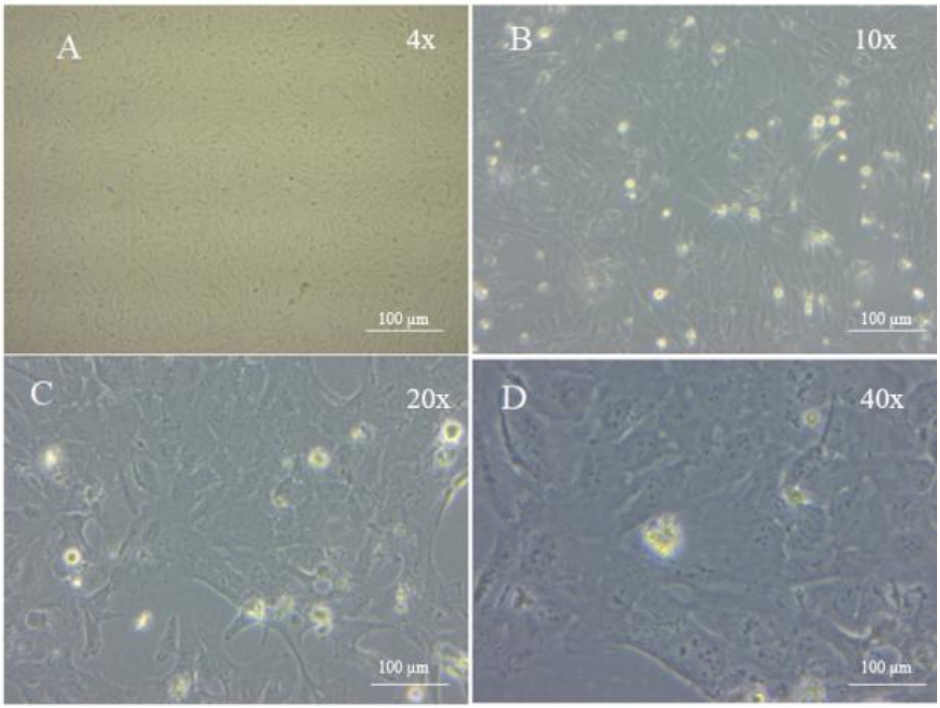

Figure 4.2 : SVG p12 Cell Line imaged with Zeiss Primovert Microscope in bright field mode A) with 4x B) 10x C) 20x D) 40x magnification.

The neuroblastoma cell line was cultured with the recommended F12:EMEM medium until the end of the experiments. However, after the 10^{th} passage, astrocyte cells continued to be cultured with DMEM medium since their growth was prolonged with EMEM medium. The growth rate with DMEM medium was considerably faster than with EMEM medium. These imaging studies were done to confirm cell line morphology and health.

4.2 Cloning and Labeling Studies

In this study, the SPOCK1 gene was ordered from DNAFORM, Japan, in pBlueScriptR plasmid. It is a phagemid vector, and the SPOCK1 gene is between 5' SalI-XhoI/BamHI 3' restriction sites. We cloned the gene into pcDNA 3.1 (-) for compatibility.

4.2.1 Cloning SPOCK1 to Mammalian Expression Vector pcDNA 3.1(-)

The pBlueScript R vector containing cells were streaked on an agar plate with Ampicillin. Then, colonies were picked, and plasmid DNA was isolated and run on a 0.9 % agarose gel to confirm sizes. GeneRuler DNA Ladder(Thermo Scientific Catalog Number SM1173) was used as a size marker (Figure 4.3).

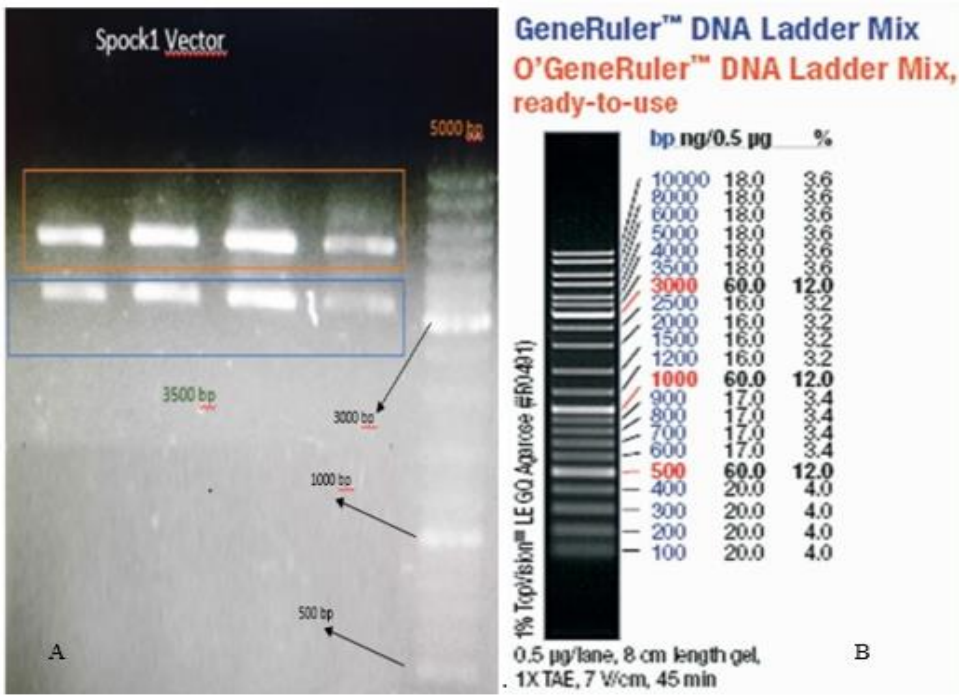

Figure 4.3 : Gel image of SPOCK1 construct A) SPOCK1 size control after plasmid isolation from agar plates. B) GeneRuler DNA Ladder.

As shown in Figure 4.3, the insert size is ~3500 bp, as expected. According to this confirmation, the construct was used in further steps.

4.2.2 Construction of pcDNA 3.1(-) Carring mCherry / EGFP

While cloning the SPOCK1 gene from the pBlueScript R vector, inserted genes were amplified by PCR inserting specific cut site regions. Appendix B contains the used primers. We aimed to compare these constructs with wild type and organelle markers by tagging SPOCK1 from two different regions, the C-terminus and 31st position. These constructs were expected to be expressed in the same intracellular

compartments. N-terminus tagging was not performed because it could impair the sequence and function of the gene. Both 31st positions tagged and C-terminus tagged SPOCK1 constructs used in the experimental plan were confirmed by sequencing. In addition to structural and signaling reasons, C-terminal fusion was preferred because the 5' mRNA secondary structure can influence translation rates. C-terminal fusion and insertional tagging could help avoid changing expression levels.

The first step of tagging was the amplification of EGFP and mCherry. The primers are given in Appendix B. The cut sites for C-terminus tagging were BamHI and KpnI, and the 31st position tagging was performed after the 31st position Alanine. After amplification, the products run on a 0.9% agarose gel to confirm their sizes (Figure 4.4). GeneRuler DNA Ladder (Thermo Scientific Catalog Number SM1173) was used as a size marker.

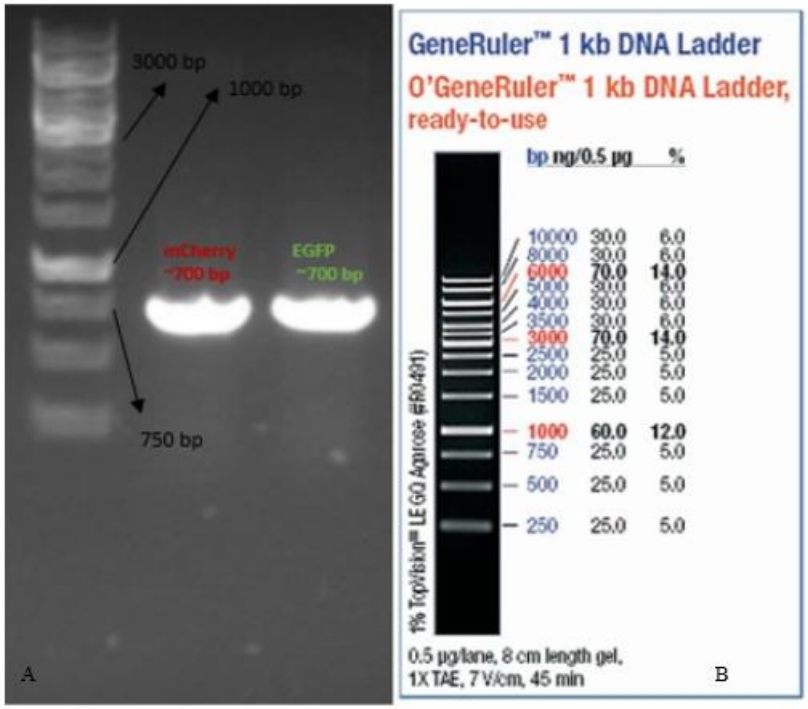

Figure 4.4 : A) Agarose gel electrophoresis images of EGFP and mCherry with GeneRuler DNA Ladder. B) GeneRuler DNA Ladder.

In order to increase the yield of the insert for ligation, a PCR purification step was added after the PCR reaction by using a GeneJet PCR Purification Kit. We used the enriched PCR product for further steps.

To clone mCherry and EGFP, we inserted the BamHI and KpnI sites by PCR.

Restricted EGFP and mCherry constructs around 720 bp were at the expected location on the gel. Ligation experiments were conducted using 1:5 and 1:10 concentrations. Amounts were calculated on the Ligation Calculator website (http://www.insilico.uni-duesseldorf.de/Lig_Input.html), which the University of Dusseldorf publishes. The related vector size was 5427 bp, EGFP was 720 bp, and mCherry was 711 bp. Ligated products were transformed into competent cells (XL-1 Blue strain *E.coli*.). Transformation experiments ended with single colony isolation. All inoculation experiments were performed with control plates. When there was growth in control, experiments were planned for inoculation for LB, accordingly. Amplified EGFP and mCherry constructs were purified, and a double digestion step was performed before ligating to pcDNA3.1(-). After ligation and plasmid isolation, control restriction step was performed. The products were loaded and run on a 0.9% gel (Figure 4.5) using GeneRuler DNA Ladder (Thermo Scientific Catalog Number SM1173) as a size marker. As the last step, gel extraction was performed with Thermo Scientific GeneJet Gel Extraction Kit.

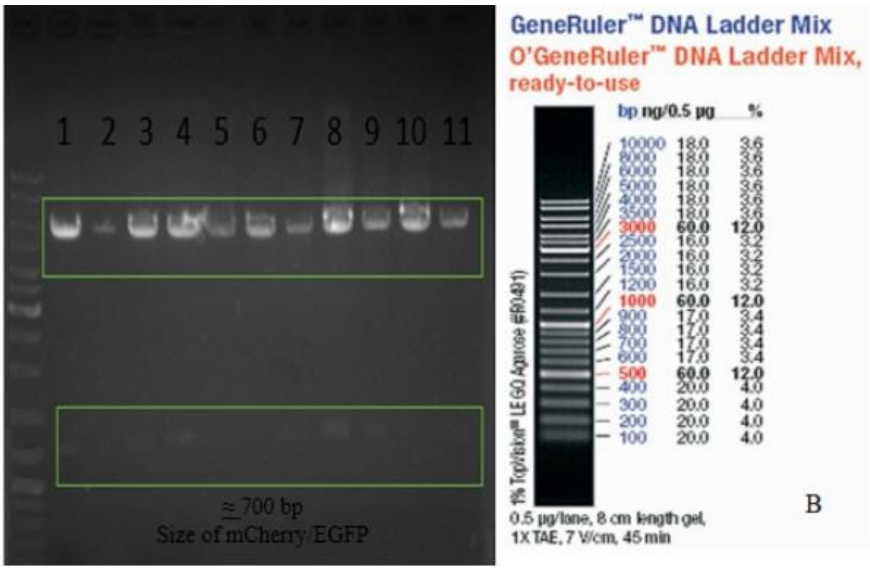

Figure 4.5 : A) Agarose gel image of double digestion EGFP and mCherry constructs and ladder GeneRuler DNA Ladder. (1-EGFP (BamHI-KpnI), 2-mCherry (BamHI-KpnI), 3-EGFP (BamHI-KpnI), 4-EGFP (BamHI-KpnI), 5-EGFP (BamHI-KpnI), 6-C Terminus Tagging Control, 7-mCherry (BamHI-KpnI),8-EGFP (BamHI-KpnI), 9-

EGFP (BamHI-KpnI), 10-mCherry (BamHI-KpnI), 11-mCherry (BamHI-KpnI)) B) GeneRuler DNA Ladder.

After this step, the EGFP and mCherry tagged pcDNA 3.1 were obtained. Restricted EGFP (720 bp) and mCherry (711 bp) constructs were at the expected location on the gel. These constructs were used for transfection experiments.

4.2.3 Tagging SPOCK1 gene from C-terminus via Cut/Paste

SPOCK1 in pBlueScript was used as a template, and related primers for these amplifications are given in Appendix B.

This amplified product, EGFP-pcDNA 3.1(-), and mCherry-pcDNA 3.1(-) were treated with XbaI and BamHI before the ligation step. After ligation, ligated products were transformed into competent cells (XL-1 Blue strain *E.coli*). Transformation experiments ended with single colony isolation. The concentration of SPOCK1-EGFP (C-Terminus) was 229.9 ng/µL, and SPOCK1-mCherry (C-Terminus) was 236.1 ng/µL. Control restriction sides for these constructs were XbaI and KpnI. The products were loaded and run on a 0.9 % gel with GeneRuler DNA Ladder (Thermo Scientific Catalog Number SM1173) as a size marker (Figure 4.6 & Figure 7).

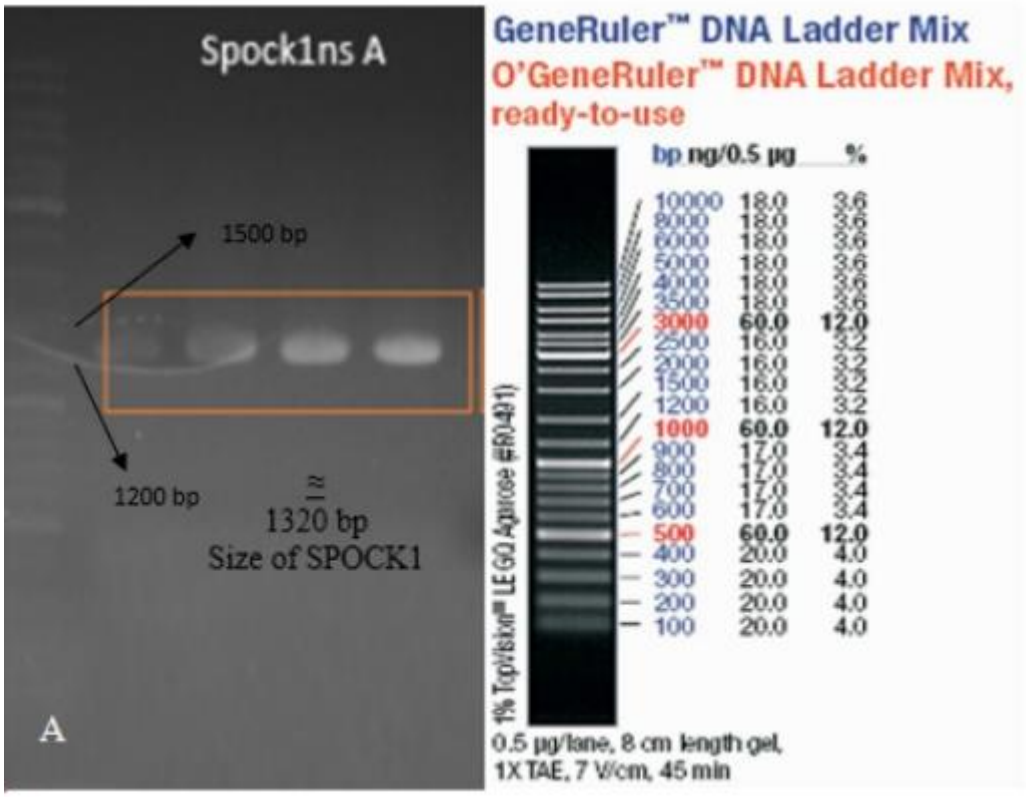

Figure 4.6 : A) SPOCK1 amplification agarose gel image. B) GeneRuler DNA Ladder.

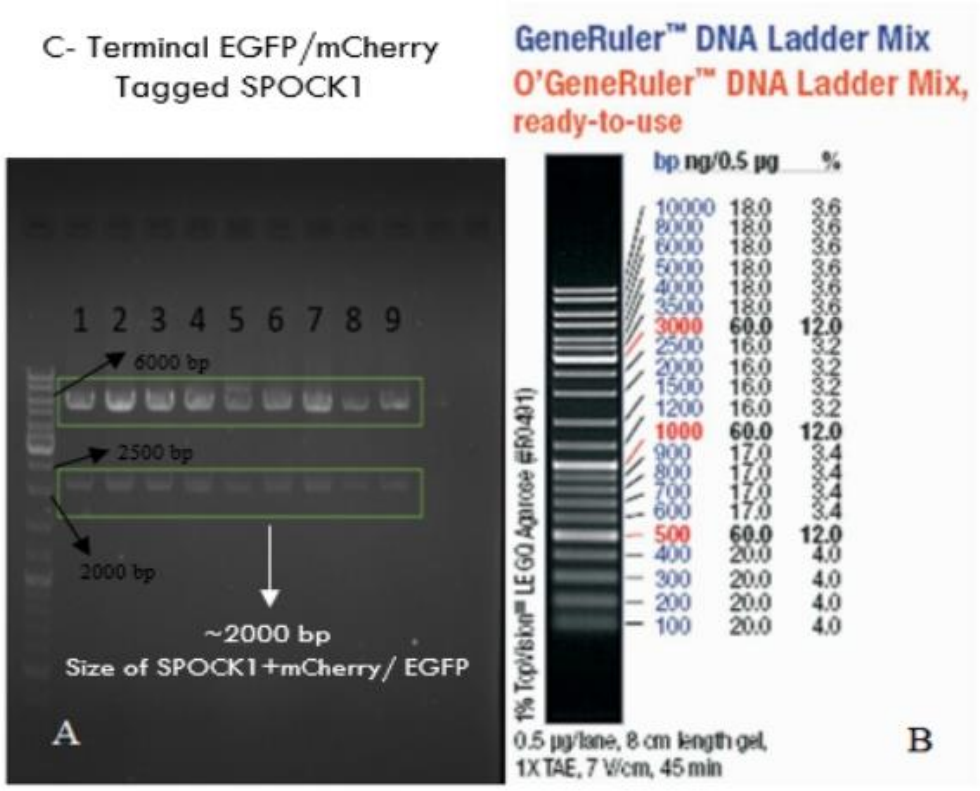

Figure 4.7 : A) Agarose gel image of double digestion of SPOCK1-EGFP and SPOCK1-mCherry constructs. (1-SPOCK1-EGFP (XbaI-KpnI), 2-SPOCK1-EGFP (XbaI-KpnI), 3-SPOCK1-EGFP (XbaI-KpnI), 4-SPOCK1-mCherry (XbaI-KpnI), 5-SPOCK1-mCherry (XbaI-KpnI), 6-SPOCK1-mCherry (XbaI-KpnI), 7-SPOCK1-mCherry (XbaI-KpnI), 8-SPOCK1-mCherry (XbaI-KpnI), 9-SPOCK1-mCherry (XbaI-KpnI)) B) GeneRuler DNA Ladder.

Restricted SPOCK1-EGFP (1320+720 bp) and SPOCK1-mCherry (1320+711 bp) constructs around 2000 bp were at the expected location on the gel. These constructs were used for transfection experiments.

4.2.4 Tagging SPOCK1 Gene from 31st Position via PCR Integration

SPOCK1 in pBlueScript was used as a template, and related primers for these amplifications are given in Appendix B. PCR, in which EGFP and mCherry without stop codon were used as templates with given primers in Appendix B, was performed. After purification, PCR products which are now named Mega Primer were used in 2nd PCR. It takes about 4 hours to amplify the whole plasmid containing SPOCK1 with these mega primers. Then, DpnI digestion was performed on half of the solution. The

solution not treated with DpnI was aimed to be used as a control for the transformation step. Only when its recognition site is methylated does DpnI cleave. This treatment aims to get rid of the unlabeled template plasmids. Ligated products were transformed into competent cells (XL-1 Blue strain *E.coli*.) Transformation experiments ended with single colony isolation. The concentration of SPOCK1-EGFP (31st position) was 112.0 ng/µL, and SPOCK1-mCherry (31st position) was 108.7 ng/µL. Control restriction sides for these constructs were XbaI and BamHI. The products were loaded and run on a 0.9% gel with GeneRuler DNA Ladder (Thermo Scientific Catalog Number SM1173) as a size marker (Figure 4.8). 1320 + 711 bp and 1320 + 720 bp of SPOCK1 was confirmed.

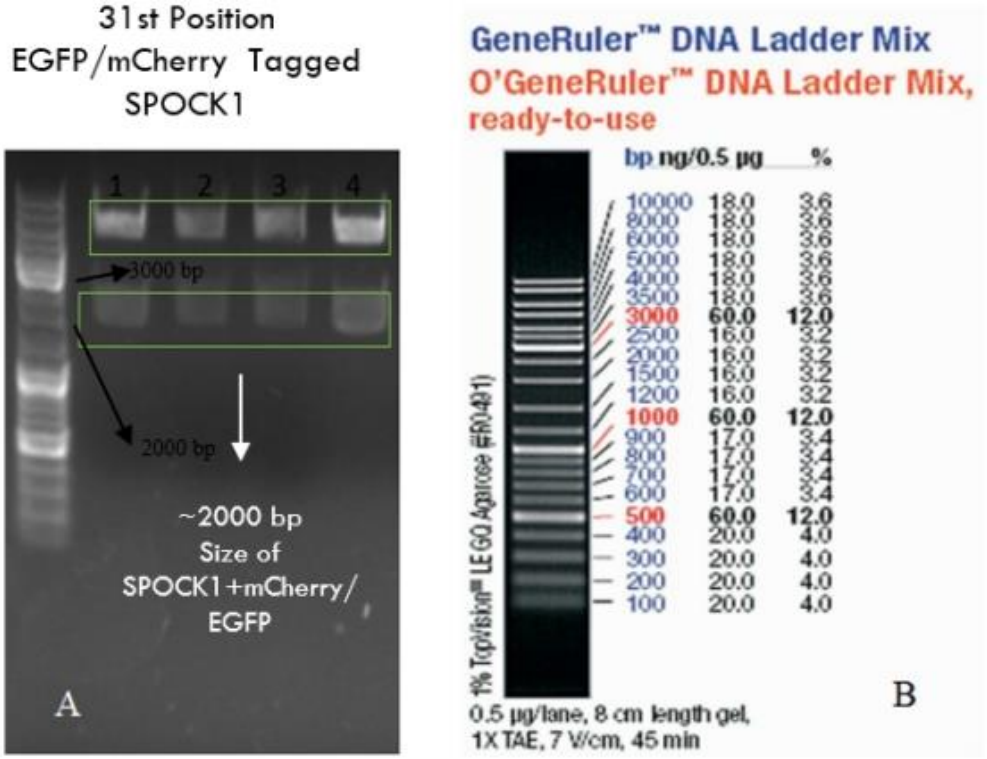

Figure 4.8 : A) Agarose gel image of double digestion of SPOCK1-EGFP (31st position) and SPOCK1-mCherry (31st position) constructs. (1-EGFP SPOCK1 (BamHI-XbaI), 2-EGFP SPOCK1 (BamHI-XbaI), 3-mCherry SPOCK1 (BamHI-XbaI), 4-mCherry SPOCK1 (BamHI-XbaI)) B) GeneRuler DNA Ladder.

Restricted SPOCK1-EGFP (1320+720 bp) and SPOCK1-mCherry (1320+711 bp) from pcDNA 3.1(-) constructs around 2000 bp were at the expected location on the

gel. These constructs were used for transfection and imaging studies experiments. While designing the primers, the stop codon of SPOCK1 was deleted for C-terminus tagging, and EGFP or mCherry sequences were added successively. Likewise, in the 31st position labeling, the stop codons of EGFP and mCherry were deleted and integrated into the SPOCK1 sequence. These constructs were also confirmed by sequencing.

4.3 Imaging Studies

In order to determine the location of the SPOCK1 gene product in the cell, cells containing a specific organelle marker labeled with fluorescent proteins were used. The cells were prepared for the endoplasmic reticulum (ER), Golgi, and mitochondria. We also used nuclear staining to check possible nuclear localization.

After transfection with these constructs, imaging was performed. mEmerald-Sec61b for ER, SiT-EGFP for Golgi, and Mito-EGFP for mitochondria were used to identify the localization of the SPOCK1 protein in the cell. Labeling from the 31st position and labeling from C-terminus were carried out. To find the localization of wild-type (untagged) SPOCK1 proteins in cells, different organelle markers and tagged SPOCK-1 constructs were carried out.

4.3.1 31st Position EGFP and mCherry Tagged SPOCK1

mCherry and EGFP constructs were used for 31st position tagging experiments. Figure 4.9 were obtained when the SPOCK1 gene was tagged from its 31st position with EGFP and mCherry. The figures show that SPOCK1 proteins were localized as punctate structures in the cytoplasm when tagged from the 31st position.

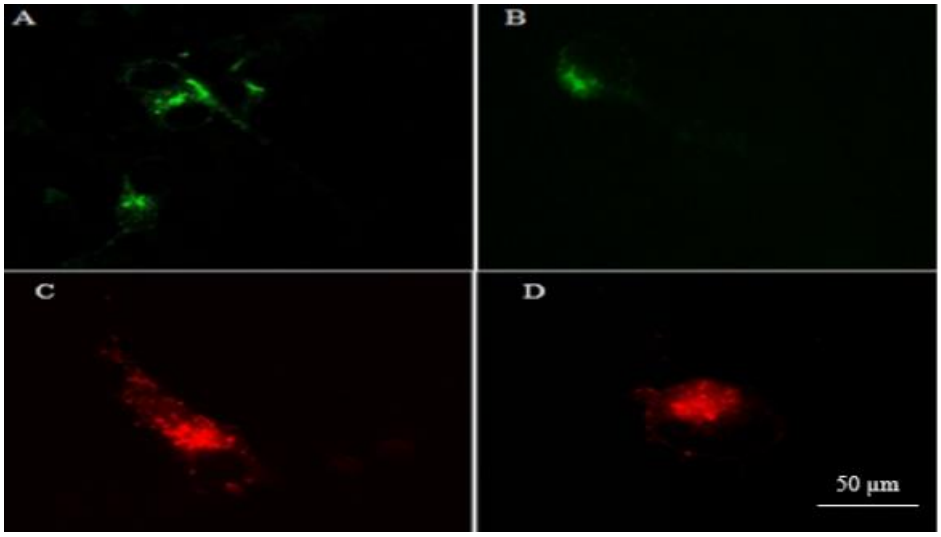

Figure 4.9 : 31st Position Tagged EGFP/mCherry-SPOCK1 **A**) SH-SY5Y cells excited with 488 nm. B) SVG p12 cells excited with 488 nm 63x objective used for imaging. C) 31st Position Tagged mCherry-SPOCK1 single transfection SH-SY5Y on cell excited with 561 nm with 63x. D) 31st Position Tagged mCherry-SPOCK1 single transfection on SVG p12 cells excited with 561 nm with 63x.

4.3.2 C-Terminus EGFP/mCherry Tagged SPOCK1

The below figures 4.10 were obtained when the SPOCK1 gene was tagged from its C-terminus. These figures show that SPOCK1 proteins were found in punctate structures in the cytosol, similar to the 31st position tagged version. This gives information that transcription can continue through the gene to the stop codon of the C-terminus EGFP and mCherry. For C-terminal tagged SPOCK1, in SVG, p12 cells had a spongy appearance and were hollow in the middle. However, SH-SY5Y cells show more distributed expression throughout the cell.

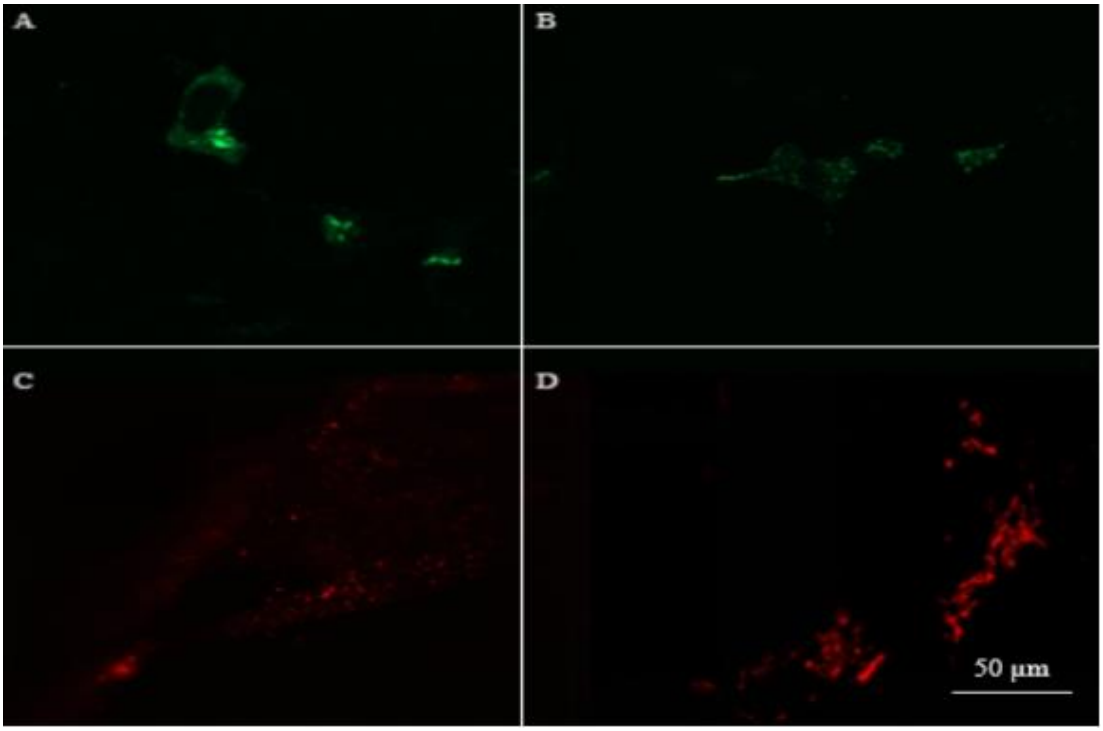

Figure 4.10 : : C-Terminal Tagged EGFP/mCherry-SPOCK1 A) C-Terminal Tagged EGFP-SPOCK1 single transfection on SH-SY5Y cells at 488 nm with 63x. B) C-Terminal Tagged EGFP-SPOCK1 single transfection on SVG p12 cells at 488 nm with 63x. C) C-Terminal Tagged mCherry-SPOCK1 single transfection on SVG p12 cells at 561 nm with 63x. & D) C-Terminal Tagged mCherry-SPOCK1 single transfection on SH-SY5Y cells at 561 nm with 63x.

These figures show that SPOCK1 proteins were found in cellular compartments. These results showed that the constructs could be expressed in the cells used in the study without a problem.

4.3.3 C-Terminus mCherry Tagged SPOCK1 & 31st Position EGFP Tagged SPOCK1 Double Transfection

This step aims to show that labeling from different places does not cause deterioration in the SPOCK1 structure and signal sequence. Figures 4.11 & 4.12 were obtained from double transfection of the SPOCK1 gene was tagged from its C-terminus with mCherry and 31st position with EGFP. As expected, position 31 tagging and C-terminus tagging constructs mostly colocalized in the same pattern. These figures show that SPOCK1 proteins were found in cellular compartments. This gives information that transcription can continue through the gene to the stop codon of the C-terminal

mCherry. In general, the mCherry-labeled constructs show a dispersed structure within the cell. The signal intensity was lower compared to EGFP-tagged constructs.

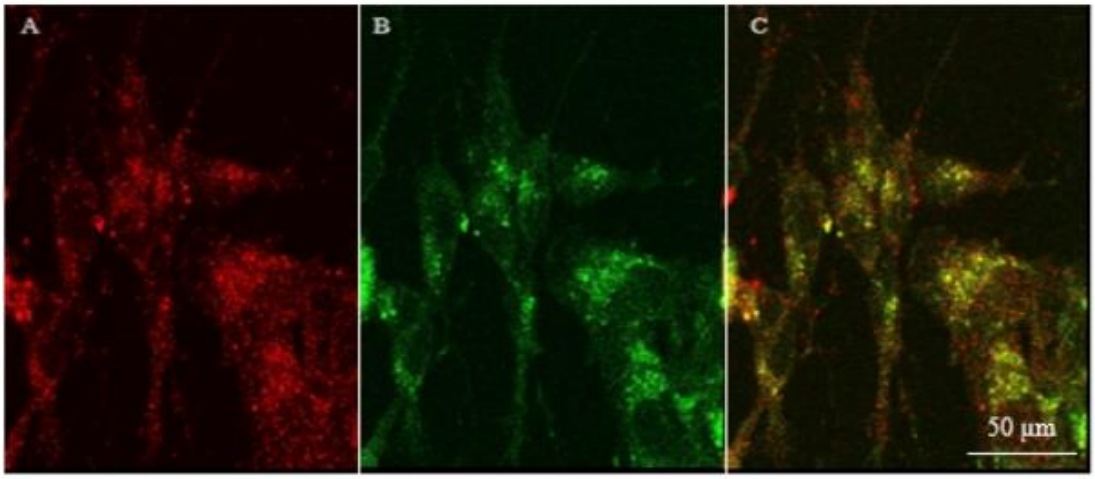

Figure 4.11: C-Terminal Tagged mCherry vs 31st Position EGFP on SH-SY5YA) C-Terminal Tagged mCherry-SPOCK1(red) transfection on SH-SY5Y Cell at 561 nm with 63x. B) 31st Position Tagged EGFP SPOCK1 transfection on SH-SY5Y Cell at 488 nm with 63x. C) Merge of A & B.

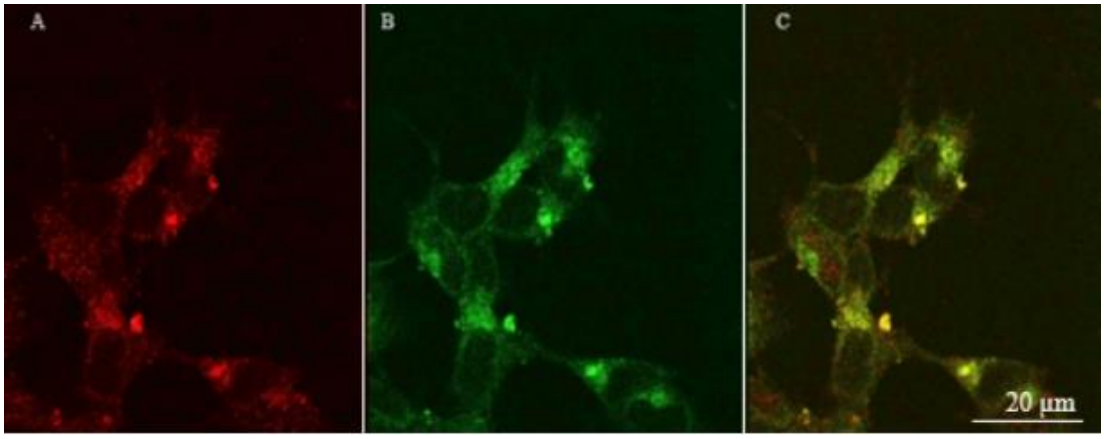

Figure 4.12 : C-Terminal Tagged mCherry vs 31st Position EGFP on SVG p12 A) C-Terminal Tagged mCherry-SPOCK1(red) transfection on SVG p12 Cell at 561 nm with 63x. B) 31st Position Tagged EGFP SPOCK1 transfection on SVG p12 Cell at 488 nm with 63x. C) Merge of A & B.

Reverse labeling of the 31st position and C-terminus tagged constructs were also performed, and similar results were observed.

4.4 Immunohistochemistry Staining

4.4.1 Wild type SPOCK1 vs. Tagged Constructs

In immunohistochemistry studies, we used SPOCK1 antibody (Ab) in neuroblastoma (SH-SY5Y) and astroglia (SVG p12) cell lines in order to compare the intracellular localization of the wild type and tagged SPOCK1. This step was done to investigate whether there is a difference between tagged constructs and wild type. Figures 4.13, 4.14, 4.15 & 4.16 show transfection studies with immunohistochemistry. Because the secondary antibody requires excitation with 488 nm, 31st position mCherry tagged SPOCK1, and C-terminal mCherry tagged SPOCK1 constructs were used for this part. Colocalization was observed as expected, indicating tagged receptors traffic similarly and localize in the same organelle with the wild-type SPOCK1.

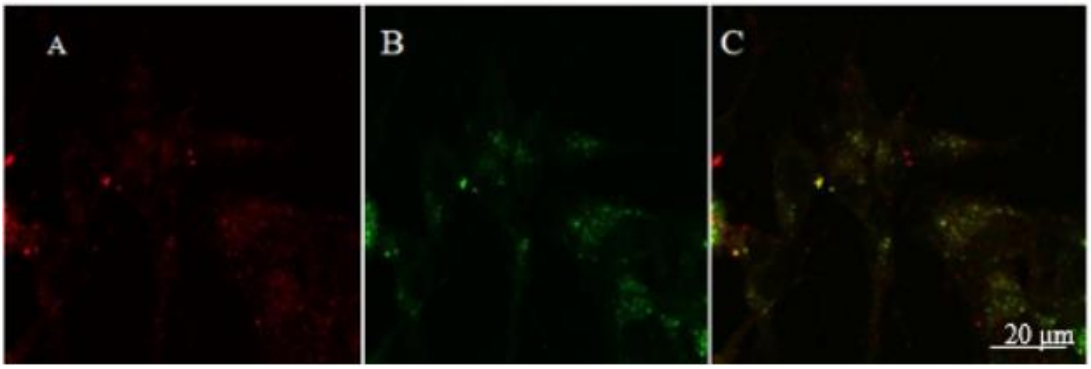

Figure 4.13 : SPOCK1 Antibody vs C-Terminal Tagged SPOCK1 on SH-SY5Y SPOCK1 Antibody (Primary Ab 1:200, Secondary Ab 1:5000) and SPOCK1-mcherry (C terminus tagging) in the SH-SY5Y neuroblastoma cell line. A) SPOCK1-mCherry (C terminus tagging) (Red), B) SPOCK1 Antibody (Green), C) SPOCK1-mCherry (C Terminus tagging) +SPOCK1 Antibody. Excitations were 481 nm and 561 nm with 63x.

When we examined the images obtained when wild-type (green) and C-terminus tagged constructs (mCherry) were thrown into the neuroblastoma cell line at the same time, the green signal and the red signal overlapped. So, we observed that the localization of wild-type and tagged constructs overlapped.

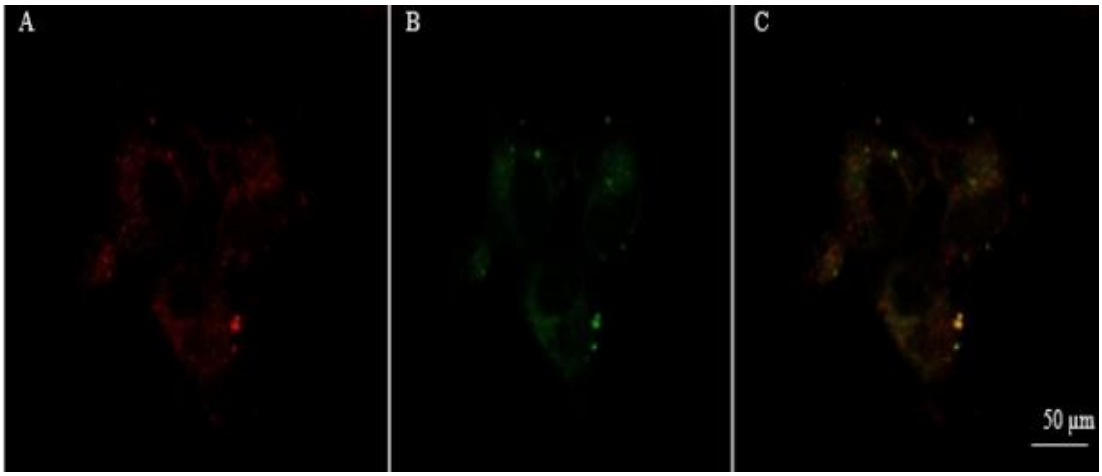

Figure 4.14 : SPOCK1 Antibody vs C-Terminal Tagged SPOCK1 on SVG p12 SPOCK1 Antibody (Primary Ab 1:200, Secondary Ab 1:5000) and SPOCK1-mcherry (C terminus tagging) in the SVG p12 astrocytes cell line. A) SPOCK1-mCherry(C terminus tagging) (Red), B) SPOCK1 Antibody (Green), C) SPOCK1-mCherry (C Terminus tagging) +SPOCK1 Antibody. Excitations were 481 nm and 561 nm with 63x.

Similar to the results we obtained in neuroblastoma cells, the localization of wild type and C-terminus tagged constructs overlapped in astrocytes.

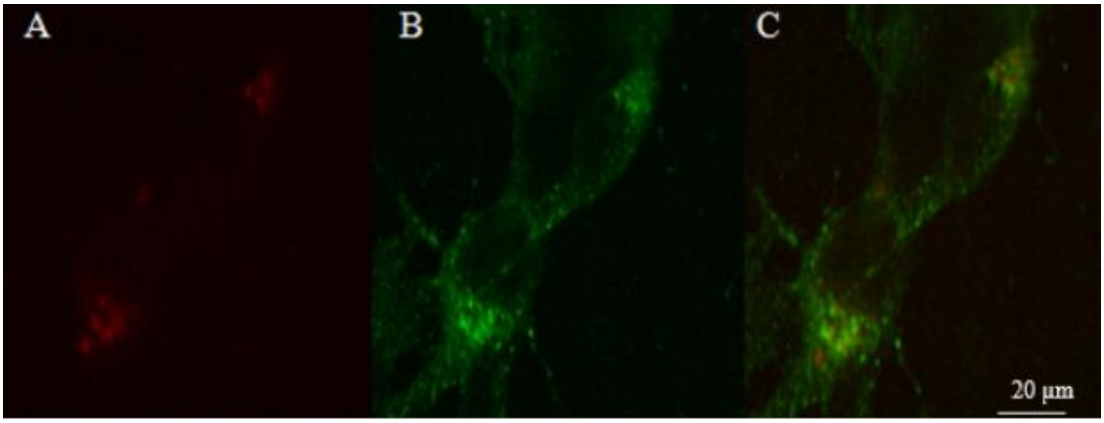

Figure 4.15: SPOCK1 Antibody vs 31st position Tagged SPOCK1 on SH-SY5Y SPOCK1 Antibody (Primary Ab 1:200, Secondary Ab 1:5000) and SPOCK1-mcherry (31st position tagging) in the SH-SY5Y neuroblastoma cell line. A) SPOCK1-mCherry (31st position tagging) (Red), B) SPOCK1 Antibody (Green), C) SPOCK1-mCherry (C Terminus tagging) +SPOCK1 Antibody. Excitations were 481 nm and 561 nm with 63x.

Imaging studies with 31st position-tagged constructs gave the same results as position C-terminus tagged constructs.

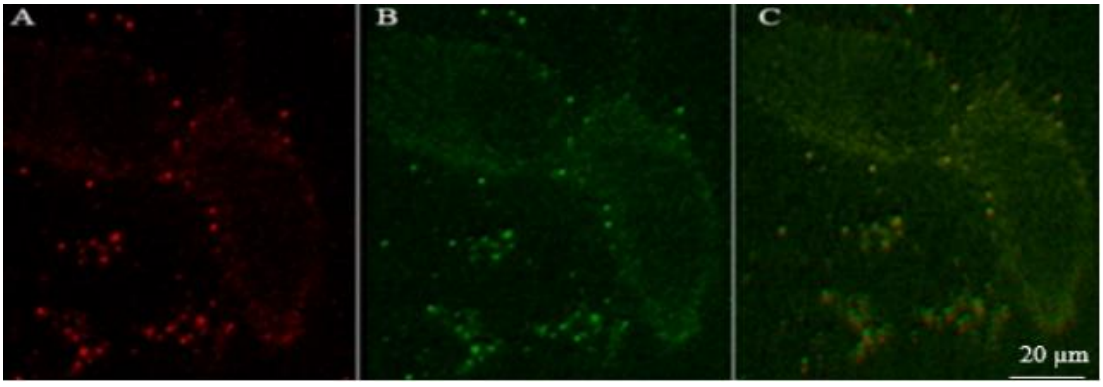

Figure 4.16: SPOCK1 Antibody vs 31st position Tagged SPOCK1 on SVG p12 SPOCK1 Antibody (Primary Ab 1:200, Secondary Ab 1:5000) and SPOCK1-mcherry (31st position tagging) in the SVG p12 astrocytes cell line. A) SPOCK1-mCherry (31st position tagging) (Red), B) SPOCK1 Antibody (Green), C) SPOCK1-mCherry (C Terminus tagging) +SPOCK1 Antibody. Excitations were 481 nm and 561 nm with 63x.

For both cell lines, 31st position/C terminus tagged constructs was observed overlapping with wild type SPOCK1.

4.4.2 Nucleus Staining

While investigating the intracellular location of SPOCK1, we prepared cell lines with stained or labeled organelles before the imaging studies. Nucleus staining was done using DRAQ. SPOCK1 protein is highly expressed in neuroblastoma (SH-SY5Y) and astroglia (SVG p12) cells. Figure 4.17 & 4.18 shows successful immunohistochemistry results with SPOCK1 antibody and DRAQ5 staining.

These images were taken with a wide-field fluorescent microscope during the preliminary experiments to optimize the SPOCK1 antibody. However, as the counterstaining for the nucleus and antibody labeling for SPOCK1 were not overlapping, we conclude that SPOCK1 is not localized in the nucleus. Since no co-localization was detected in the nucleus, this experiment was not repeated under the confocal microscope.

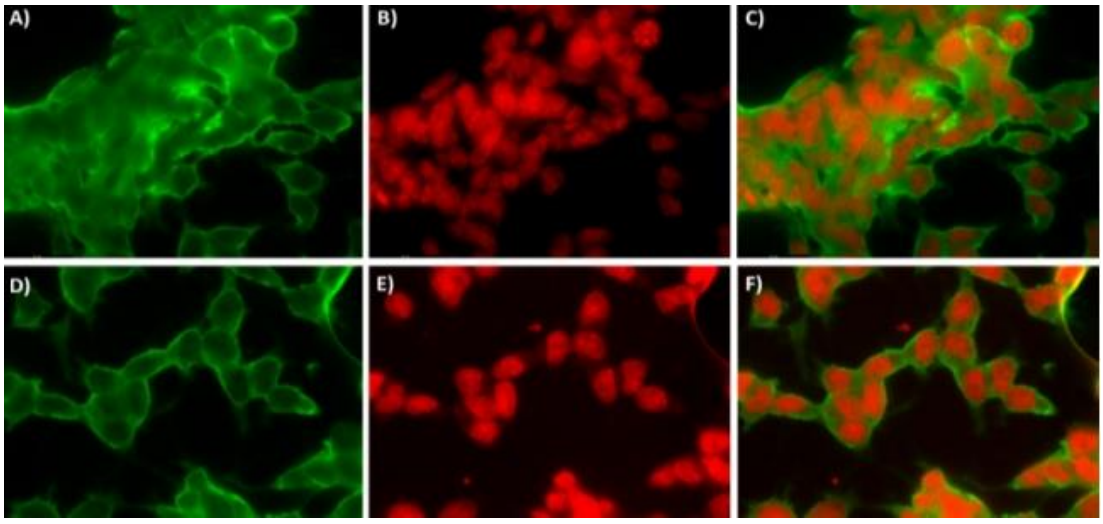

Figure 4.17: SPOCK1 (Primary Ab 1:200, Secondary Ab 1:1000) and nucleus (DRAQ5) in the SH-SY5Y neuroblastoma cell line. A&D) SPOCK1 (Green), B&E) Nucleus(Red), C&F) SPOCK1+Nucleus. Excitations were 405 nm and 561 nm with 63x.

In the astrocyte cell line, we repeat the immunohistochemistry experiments with nucleus staining. We obtained similar results, indicating that SPOCK1 is not localized in the nucleus of these cells.

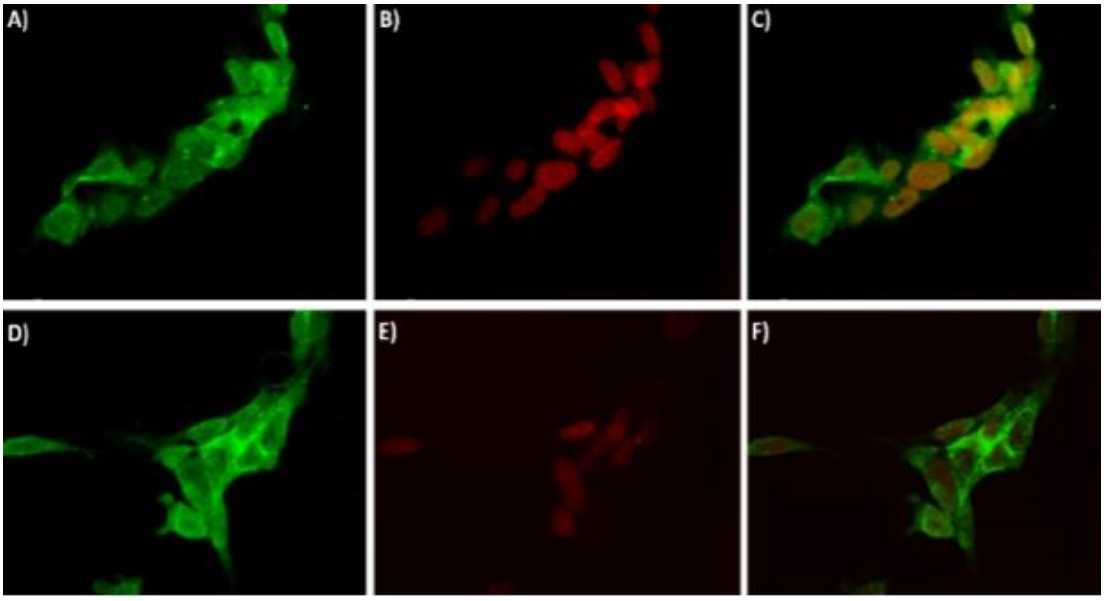

Figure 4.18 : SPOCK1 (Primary Ab 1:200, S 1:200, Secondary Ab 1:1000) and nucleus (DRAQ5) in the SVG p12 astrocytes cell line. A&D) SPOCK1 (Green), B&E) Nucleus (Red), C&F) SPOCK1+Nucleus. Excitations were 405 nm and 561 nm with 63x.

As can be seen in these figures, SPOCK1 expression is relatively high, even in different nerve cells. The neuroblastoma cell expression suggests a more porous structure than astrocytes. Also, neuroblastoma cells colonized more spherically, resulting in imaging difficulties.

4.5 Organelle Markers

4.5.1 Endoplasmic Reticulum Marker

The SPOCK1 is described as a secretory protein in Protein Atlas. Since the endoplasmic reticulum is involved in secretory pathways, we checked whether SPOCK1 is in this organelle with imaging studies. Expression was expected in the endoplasmic reticulum since it is also involved in the extracellular matrix. So,

according to this info, mEmerald-Sec61b is expressed with mCherry-SPOCK1 C-terminus or 31st position tagged. However, as seen in Figures 4.3.19 & 4.3.20, colocalization was not detected.

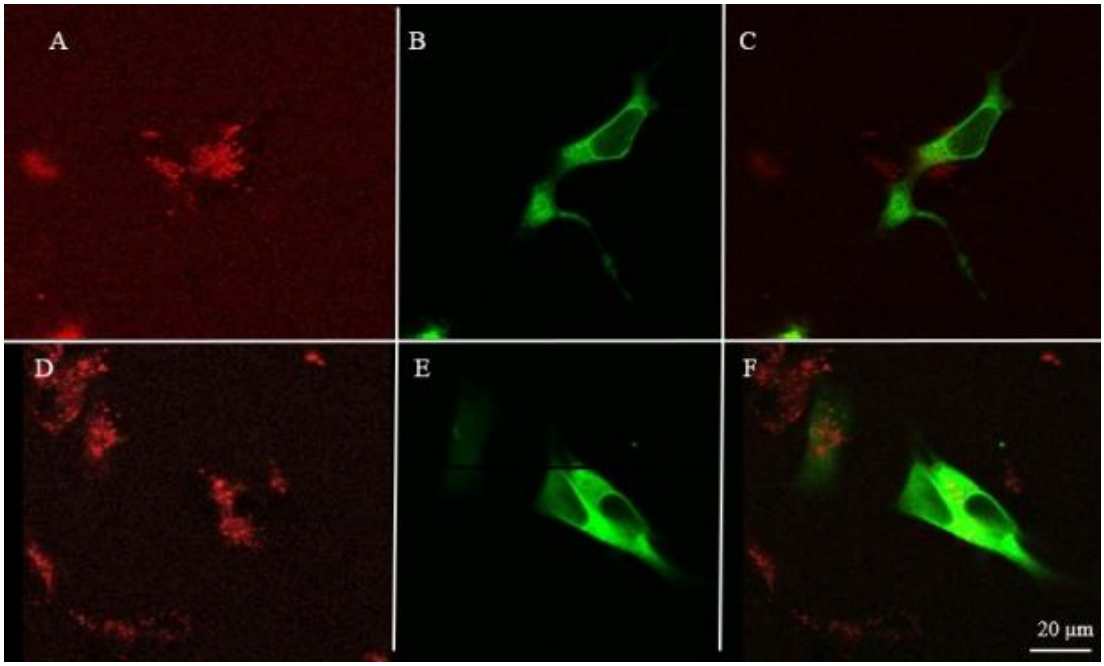

Figure 4.19 : mCherry SPOCK1 vs ER Marker on SH-SY5Y A) mCherry SPOCK1(Red) Transfection on SVG p12 cell at 561 nm with 63x. B) ER Marker mEmerald-Sec61b (Green) Transfection on SVG p12 cell at 488 nm with 63x. C) Merge of A & B.D) mCherry SPOCK1 transfection on SH-SY5Y cell (Red) at 561 nm with 63x E) ER Marker mEmerald-Sec61b (Green) transfection on SH-SY5Y cell at 488 nm with 63x. F) Merge of D & E.

C-terminally tagged mCherry, and ER marker mEmerald-Sec61b were not shown to have colocalization results for both cell lines.

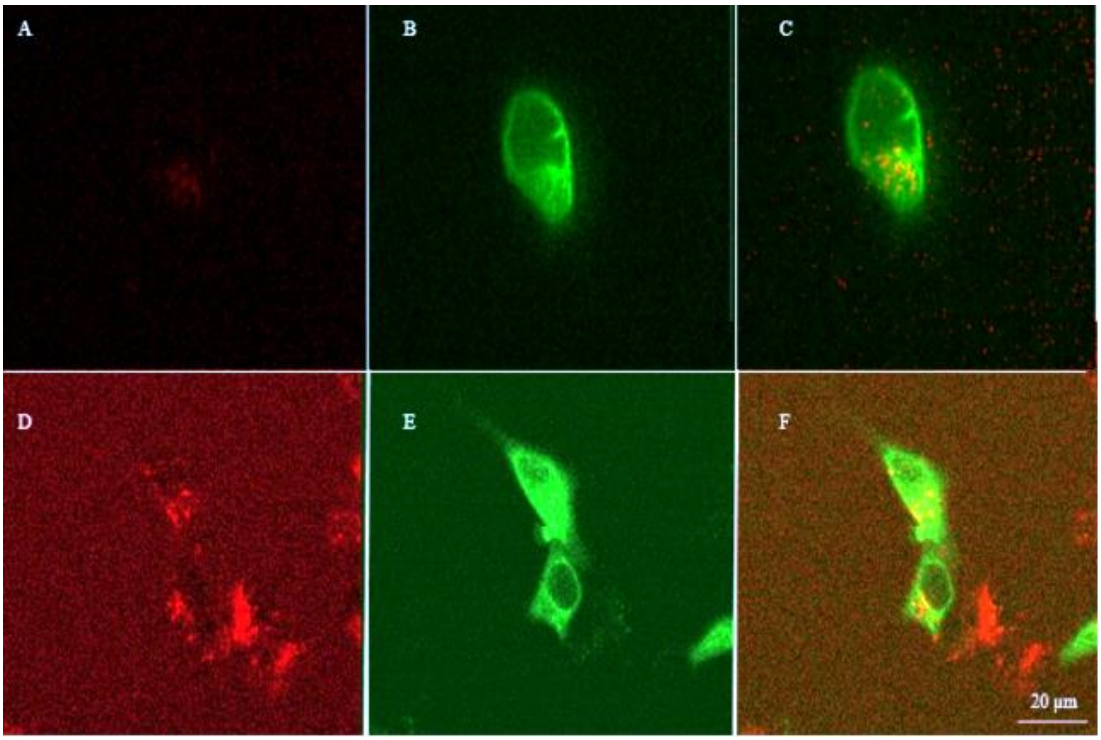

Figure 4.20 : mCherry SPOCK1 vs ER Marker on SVG p12 A) mCherry SPOCK1 (31st position tagging) (Red) transfection on SVG p12 cell at 561 nm with 63x. B) ER Marker mEmerald-Sec61b (Green) transfection on SVG p12 cell at 488 nm with 63x. C) Merge of A & B. D) mCherry SPOCK1 (31st position tagging) (Red) transfection on SH-SY5Y cell at 561 nm with 63x E) ER Marker mEmerald-Sec61b (Green) Transfection on SVG p12 cell at 488 nm with 63x. F) Merge of D & E

As expected, similar results were obtained with C-terminal tagging. Colocalization was not detected in either cell line between the 31st position labeled SPOCK1 and the ER organelle marker.

4.5.2 Golgi Marker

The structure of SPOCK1 has previously been described. GAGs are covalently attached to the core proteins of proteoglycans. Heparin sulfate proteoglycan is involved in various functions ranging from structure maintenance and development to ECM establishment and basement membrane formation via adhesion to matrix molecules. Heparin sulfate, in particular, functions as a co-receptor to regulate cell-cell interactions for various cell surface receptors, thereby influencing cell-ECM

interactions. Heparin sulfate proteoglycan also regulates cell migration and adhesion, differentiation, proliferation, angiogenesis, and morphogenesis, as well as the cytoskeletal organization and tissue repair (Mythreye & Blobe, 2010).

Because of its modular structure, SPOCK1 can be classified as an ECM regulator and may interact with the cell surface. Thus, one of the first questions we sought to answer was whether it was localized in the Golgi. This question was answered by simultaneous transfection of the mCherry-tagged SPOCK1 gene and the Golgi marker SiT-EGFP constructs. SiT-EGFP has mEGFP site in the plasmid map, which can be found in Appendix C. Colocalization was not detected when the co-transfected cells were imaged, as seen in Figures 4.21 & 4.22.

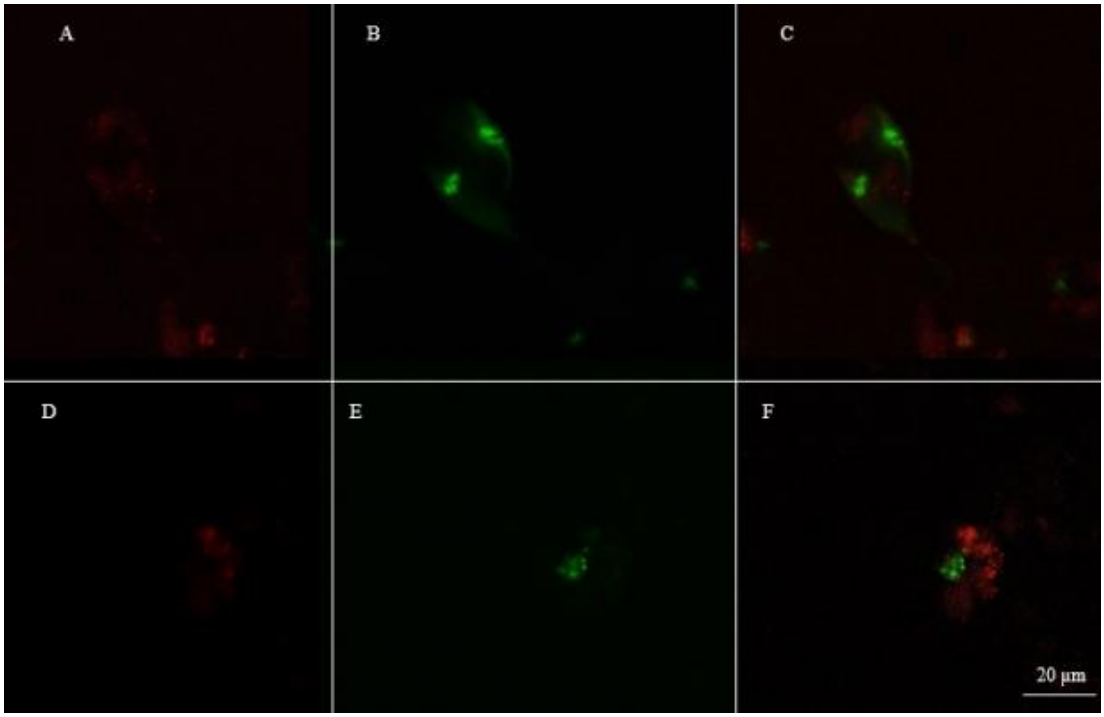

Figure 4.21: mCherry SPOCK1 vs Golgi Marker on SH-SY5Y A) mCherry SPOCK1 transfection on SH-SY5Y Cell at 561 nm with 63x. B) Golgi Marker SiT-EGFP (Green) transfection on SH-SY5Y Cell at 561 nm with 63x. C) Merge of A & B. D) mCherry SPOCK1(Red) transfection on SVG p12 cell at 561 nm with 63x. E) Golgi Marker SiT-EGFP (Green) transfection on SVG p12 cell at 488 nm with 63x. F) Merge of D & E.

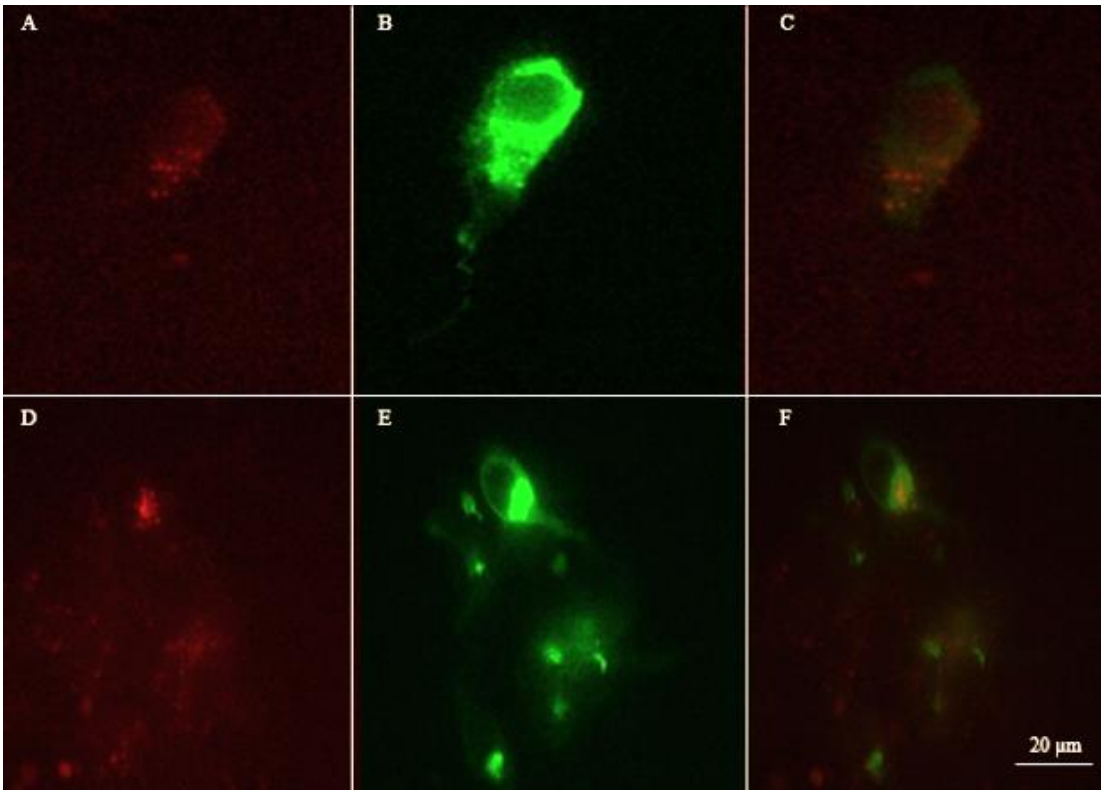

Figure 4.22: mCherry SPOCK1 vs Golgi Marker on SVG p12 A) mCherry SPOCK1 (31st position tagging) transfection on SVG p12 Cell at 561 nm with 63x. B) Golgi Marker SiT-EGFP (Green) transfection on SH-SY5Y Cell at 561 nm with 63x. C) Merge of A & B. D) mCherry SPOCK1 (31st position tagging) transfection on SH-SY5Y Cell at 561 nm with 63x. E)Golgi Marker SiT-EGFP (Green) transfection on SH-SY5Y Cell at 561 nm with 63x. F) Merge of D & E.

4.5.3 Mitochondria Markers

In a recent (February 2022) published study, SPOCK1, an extracellular proteoglycan, was progressively recognized as a factor in cancer development and progression. Investigation of how SPOCK1, which is found in low concentrations in non-tumorous hepatocytes, promotes the development and progression of malignant hepatocellular tumors was conducted. Although SPOCK1 is an extracellular matrix proteoglycan, its concentration in the cytoplasm of hepatocytes starts to rise from low concentrations in normal cells to much higher levels in cirrhotic human liver cells and hepatocellular carcinoma cells. In hepatoma cell lines, cytoplasmic SPOCK1 colocalized with mitochondrial markers such as MitoTracker and TOMM20, a characteristic protein of

the mitochondrion's outer membrane, and was found in the cell nucleus (Váncza *et al*., 2022).

Distribution of label-resembled punctate organelles, so we suspected mitochondria and tested it. While we also discovered this literature that claims SPOCK1 might be localized in mitochondria, our results agree with the current literature. The alternative experiment plans were organized. Using 31st position mCherry tagged SPOCK1, C-terminus mCherry tagged SPOCK1, and mitoEGFP (Mitochondria marker), co-transfection studies were carried out, and cells were imaged using a confocal microscope, as seen in Figures 4.23 & 4.24.

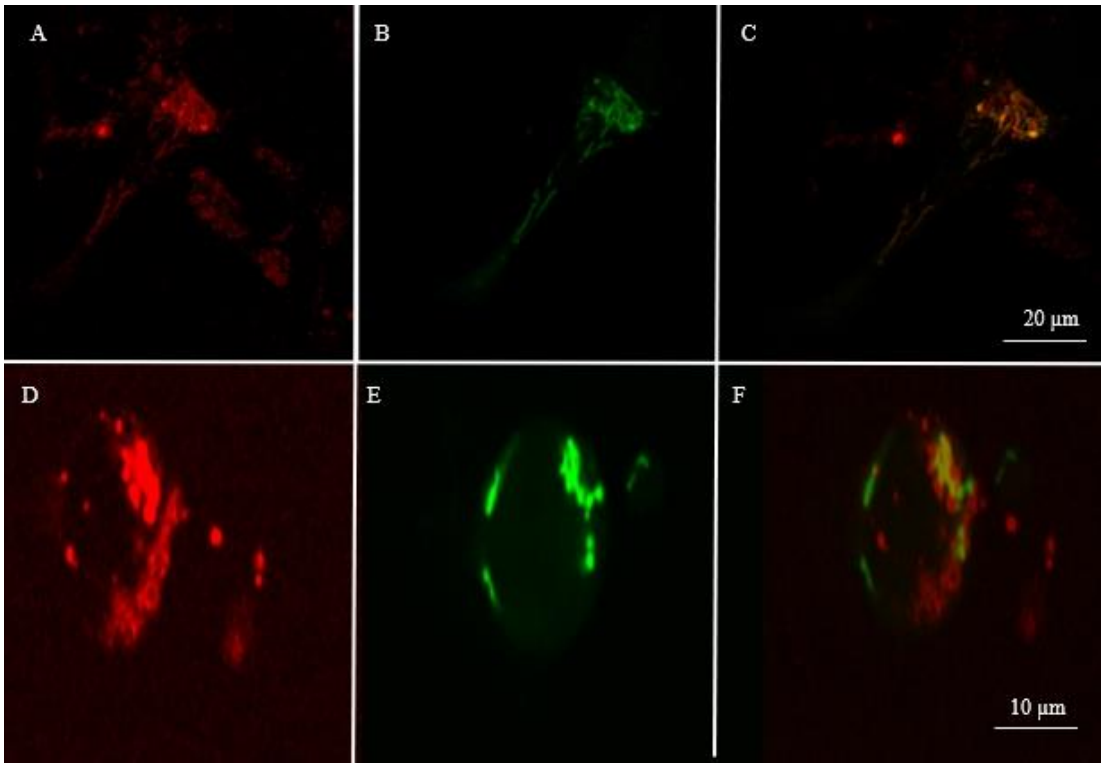

Figure 4.23 : mCherry SPOCK1 vs Mitochondria Marker on SH-SY5Y A) C-terminus mCherry transfection on SH-SY5Y at 561 nm with 63x. B) mito-EGFP transfection on SH-SY5Y at 488 nm with 63x. C) Merge of A & B. D) C-terminus mCherry transfection on SVG p12 at 561 nm with 63x E) mito-EGFP transfection on SVG p12 at 488 nm with 63x. F) Merge of D & E.

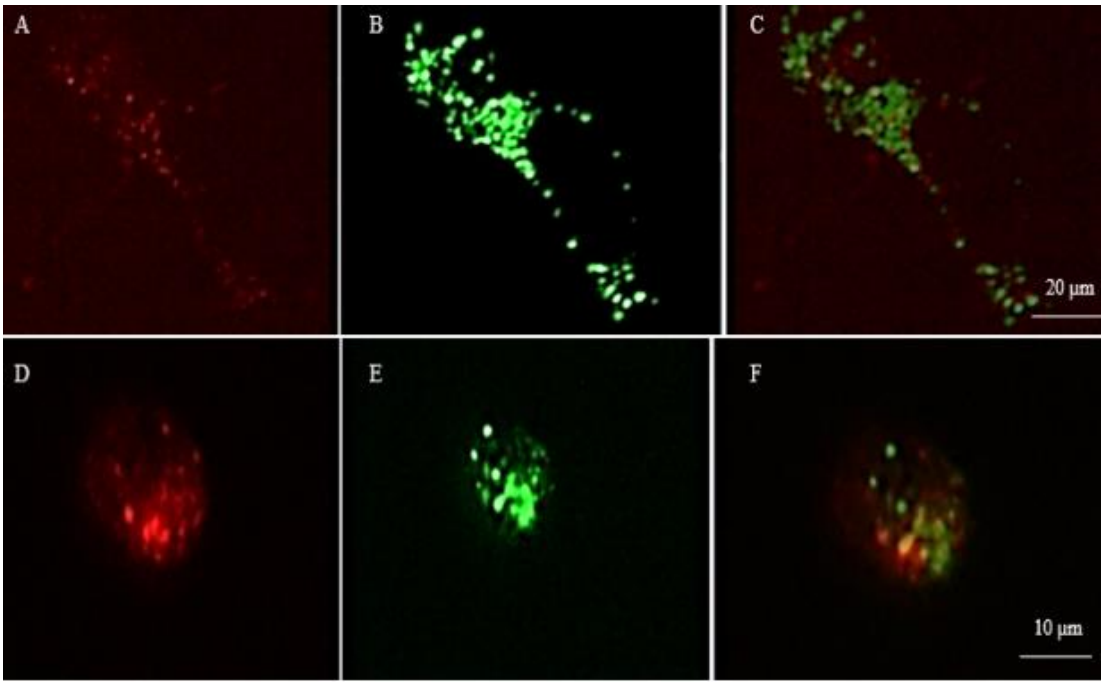

Figure 4.24: mCherry SPOCK1 vs Mitochondria Marker on SVG p12 A) 31st position mCherry transfection on SVG p12 at 561 nm with 63x B) mito-EGFP transfection on SVG p12 at 488 nm with 63x. C) Merge of A& B. D) 31st position mCherry transfection on SH-SY5Y at 561 nm with 63x. E) mito-EGFP transfection on SH-SY5Y at 488 nm with 63x. F) Merge of D & E.

These figures show the double transfection of SPOCK1 mcherry and mito-EGFP constructs. Because the granular cytoplasmic SPOCK1 reaction raised the possibility that the proteoglycan localizes in the mitochondria, neural cell lines were double transfected with 31st position mCherry tagged SPOCK1 or C-Terminal Tagged SPOCK1 and either mito-EGFP. In the SH-SY5Y cell line, mCherry-tagged proteins and mitochondria marker mito-EGFP show colocalization. Similar results were obtained for the SVG p12 cell line. Likewise, with single transfection of C-terminal mCherry tagged SPOCK1, the mCherry-labeled constructs show a dispersed structure within the cell. Similar morphology of cells and distributions of the tagged protein was observed. Mito-EGFP, a mitochondrial marker, showed the mitochondrial pattern. The morphological features of the cells are detected along with the SPOCK1 protein in the mitochondria. Figures suggest that SPOCK1 is a protein that transfers from the cytoplasm to the mitochondria.

CHAPTER 5

DISCUSSION

This study aims to determine which organelle(s) the SPOCK1 is localized in neuroblastoma and astrocytes. These findings could help us understand the possible roles of this protein in the nervous system and can help us make contributions to the development of molecular techniques for diagnosing and treating Alzheimer's disease.

In order to study the expression pattern of the localization of the SPOCK1 protein in live cells, fluorescent proteins mCherry and EGFP were used during tagging experiments. Palmer and Freeman (2004) demonstrated that in HEK293T cells, all proteins tagged with GFP at the C-terminus were correctly localized using reverse transfection microarrays. On the other hand, those tagged at the N-terminus were incorrectly localized in less than half of the cases. This finding suggests that inserting in-frame fusion tags at the N-terminus of a protein may be riskier than inserting tags at the C-terminus. So, the N-terminus tagging was not performed for explained reasons.

C-terminal tagged constructs showed dispersed expression within the cell, similar to immunohistochemistry staining. Since fluorescent proteins can destabilize tagged protein function and localization, several positions, including the 31st position and C-Terminal, tagging were performed for SPOCK1. As expected, there was no difference in intracellular localization of proteins tagged from the 31st position or C-terminus. The reason for choosing the 31st position, between Ala-Gly, instead of N-terminus tagging is because this position is just after the known signal sequence of SPOCK1. Our imaging results showed that tagging at this position did not cause a change in the trafficking or function of the protein. Wild type and tagged constructs were compared in both cell lines, and colocalization was detected. Then, studies were carried out with organelle and nucleus markers. Each construct shows an expression that indicates successful transfections.

SPOCK1, an extracellular protein in tumor tissues, showed that it plays a role in the regulation of the matrix (ECM). The endoplasmic reticulum, Golgi apparatus, and the vesicles that move between them are all included in the secretory pathway. However, in the transfection studies with C-terminal tagged SPOCK1 and Golgi/endoplasmic reticulum markers colocalization was not detected in neural cells. The maturation time of EGFP is reported as 60 min (Macdonald *et al.*, 2011). For mCherry, it is around 57 min (Merzlyak *et al.*, 2007). Thus it might be possible that possible localization of SPOCK1 in ER and/or Golgi might have been missed due to the relatively slow maturation of the fluorescent tags used in this study. With this data, we can conclude that SPOCK1 does not retain in these organelles, but we cannot conclude that they do not pass through them. In order to make this comment, we need to use a much faster maturing fluorescent protein such as Neongreen (10 min maturation time) or stop protein synthesis and trafficking and image the cells after a certain amount of time (~2hr).

Strikingly colocalization of SPOCK1 and organelle markers was only observed with the mitochondria marker—constructs viewed under a confocal microscope after transfecting into cells. Immunohistochemistry studies conducted with the wild-type SPOCK1 localization also showed a similar punctate pattern in the cytosol, indicating a mitochondrial localization and co-localized with the fluorescently tagged SPOCK1, supporting that the mitochondrial localization is not due to the limitations of the fluorescent protein maturation times.

In order to conduct complementary experiments reported in this study to further show SPOCK1 localization in mitochondria we carried out experiments with mScarlet, mitochondria marker, and C-terminal tagged EGFP-SPOCK1. Original images obtained for these studies showed one-to-one overlap. However, when we performed a single staining with mScarlet, mitochondria marker for control, we detected that mScarlet was giving signals at both 488 nm and 561 nm channels. Various concentrations of mScarlet, mitochondria marker, and different excitations were tested with no success. This marker was unsuitable for EGFP labeled SPOCK1 and thus was removed from the experimental plan.

In a biological manifestation, colocalization is defined as the presence of two or more distinct molecules in the same physical location in a specimen. Colocalization may indicate that the molecules are attached to the same receptor in the context of a tissue section, individual cell, or sub-cellular organelle viewed under a microscope. In contrast, in the context of digital imaging, the term refers to colors emitted by fluorescent molecules sharing the same pixel in the image. Microscopes and specimen preparation methods are prone to error and can produce images with unintended character traits that may be mischaracterized as belonging to the biological specimen. Furthermore, our brains are hardwired to interpret what we see quickly and with an unconscious bias toward what makes the most sense to us based on our current understanding. Unaddressed errors in microscopy images, combined with the bias we bring to visual image interpretation, can lead to incorrect conclusions and irreproducible imaging data (Jost & Waters, 2019). Thus, mScarlet, which exhibits spectral bleed-through, was extracted from experimental plans after this point to avoid false interpretations (Figure 6.11 & 6.12). Other difficulties are encountered during the cell culture studies. The first was the slow growth of SVG p12 cells with the recommended EMEM medium, especially after the 10^{th} passage. We overcame this problem by using a DMEM medium. Once the cells were revived from frozen stock, their initial growth was prolonged, and the EMEM medium could not provide the necessary content. While SH-SY5Y cells grew very slowly at the beginning of the experiments, their growth rate increased considerably after the sixth passage. The transfection efficiency within the two cell lines was low during imaging studies, even with the LTX reagent. While a rate of 80-90% was expected, most studies detected a lower efficiency of 50-60%. Different transfection reagents, such as Turbofect and Lipofectamine 2000, were also used for trial purposes. During the double transfection experiments, the size of the constructs can affect the entry of the two constructs into the cell. Small-sized constructs were more visible in imaging studies, whereas large ones were not well integrated. Constructs were transfected and imaged in another cell line, confirming no problem with the constructs. Then, different constructs created in our lab in SH-SY5Y and SVG p12 cell lines were transfected and controlled. Again, the transfection efficiency remained in the 50-60% range.

Secondly, problems were encountered due to the cells' morphological structure and viability. Loss of focus was common as the SVG p12 cells clumped together. This spherical growth also helped us see the differences between the two cell lines. SH-SY5Y cells were often imaged, including their extensions. Although we observed live, it was challenging to get an overlap image for mitochondria and SPOCK1, as the cells were alive, had active motion, and took longer than expected to take images at high exposures. The best representative images were added to this thesis.

Currently, the only literature related to SPOCK1 and the nervous system is that the SPOCK1 mRNA is found in the developing central nervous system, including the brain, retina, and spinal cord (O'Brown *et al*., 2021). A recent study showed, via immunohistochemistry, that the SPOCK1 protein is unexpectedly localized at mitochondria in hepatoma cell lines (Váncza *et al*., 2022). Our observation of colocalization of the C-terminal and 31st position tagged SPOCK1-mCherry, and the mito-EGFP construct in two different neural cell lines supported the reports on mitochondrial localization of the SPOCK1 in hepatoma cells. These observations of mitochondrial localization raised the possibility that SPOCK1 could have a currently unknown physiological function.

Mitochondria play a role in energy metabolism, regulating apoptotic pathways in the cell.Apoptosis is programmed cell death that occurs during normal development and tissue homeostasis. It is characterized by activating specific biochemical pathways that lead to the cell's destruction and its DNA's fragmentation. Apoptosis is thought to play a role in the development and function of the nervous system, as well as in the clearance of damaged or unnecessary cells. There is evidence that APP, apoptosis, and astrocytes may be interconnected in the development and progression of AD, as abnormal processing of APP may lead to the activation of apoptotic pathways in astrocytes. As astrocytes may play a role in clearing amyloid plaques through phagocytosis (the ingestion and degradation of debris), the death of these cells can lead to the formation of amyloid plaques (Kinney *et. al,* 2018). However, the exact relationship between these factors in AD development is still not fully understood, and more research is needed to determine the mechanisms involved (Guo *et*. al, 2020).

CHAPTER 6

CONCLUSION AND FUTURE PERSPECTIVE

The complicated genetic etiology of Late-Onset Alzheimer's Disease (LOAD) is currently unknown, which hinders the early and differential diagnosis of LOAD. Although the exact cause of Alzheimer's disease is unknown, amyloid formed in the brain plaques and neurofibrillary tangles have a vital role. SPOCK1 (testican-1) is suggested to modulate the endocytic pathway and lead to the accumulation of Aβ40 and Aβ42. Moreover, we have identified two variants in the SPOCK1 gene region associated with (LOAD), supported by a case/control study (Rafatova ,2022). In the light of these information,in his study, we aimed to understand the SPOCK1 protein expression pattern in neural cells and identify the intracellular localization of SPOCK1 in two different neural cell lines. Experiments were planned by using different organelle markers and antibody staining on neuroblastoma and astrocyte cells for this study. SPOCK1 antibody, C and 31st position EGFP and mCherry tagged constructs, mEmerald-Sec61b for ER; SiT-EGFP for Golgi; mito-EGFP for mitochondria staining were used to capture SPOCK1 localization in the studied cells.

Our results suggested an unexpected mitochondrial localization for SPOCK1, and this finding should be further investigated in order to understand possible unknown functions of SPOCK1 in this organelle. The main of cellular energy is produced by mitochondria, but aging or damaged mitochondria release too many free radicals, which can lower the amount of ATP available and cause energy loss and mitochondrial dysfunction in AD. Importantly, oxidative damage to the mitochondrial ATP synthase gene promoter causes lower amounts of the corresponding protein, which lowers ATP generation, causes nuclear DNA damage to genes that are susceptible to it, and leads in function loss.

As an outcome of this study, we can start understanding the molecular function of the SPOCK1 protein in neural cells. SPOCK1, among other variations linked to LOAD,

will be investigated in microglia, astroglia, and neuroblastoma cells of the nervous system based on an ongoing study by our research team and recent literature.

SPOCK1's function in neural cells needs further investigation. The BioID analysis will also be used to determine which proteins the SPOCK1 protein interacts with within these cells. Also, confirmed tagged constructs generated during this study can be used in advanced fluorescent-based studies such as FRET, BRET, and BiFC analysis for protein-protein interactions.

Observing the mitochondrial localization of SPOCK1 in neural cells can allow us to speculate on the potential role of SPOCK1 during apoptosis and propose new molecules for Alzheimer's etiology. We hope that the research that will be conducted could significantly advance the development of molecular methods for detecting and managing Alzheimer's disease.

REFERENCES

Amberger, J., Bocchini, C., & Hamosh, A. (2011). A new face and new challenges for Online Mendelian Inheritance in Man (OMIM®). Human mutation, 32(5), 564- 567.

Barrera-Ocampo, A., Arlt, S., Matschke, J., Hartmann, U., Puig, B., Ferrer, I., Zürbig, P., Glatzel, M., Sepulveda-Falla, D., & Jahn, H. (2016). Amyloid-β Precursor Protein Modulates the Sorting of Testican-1 and Contributes to Its Accumulation in Brain Tissue and Cerebrospinal Fluid from Patients with Alzheimer Disease. *Journal of neuropathology and experimental neurology*, *75*(9), 903–916. https://doi.org/10.1093/jnen/nlw065

Cantile C, Youssef S. Nervous System. Jubb, Kennedy & Palmer's Pathology of Domestic Animals: Volume 1. 2016:250–406. doi: 10.1016/B978-0-7020-5317-7.00004-7. Epub 2015 Nov 20. PMCID: PMC8142716.
Chen Q, Yao YT, Xu H, Chen YB, Gu M, Cai ZK, Wang Z. SPOCK1 promotes tumor growth and metastasis in human prostate cancer. Drug Des Devel Ther. 2016 Jul 18;10:2311-21. doi: 10.2147/DDDT.S91321. PMID: 27486308; PMCID: PMC4958368.

De Zeeuw, C. I., Hoogland, T. M. (2015). Reappraisal of Bergmann glial cells as modulators of cerebellar circuit function. Front. Cell Neurosci. 9, 246. doi: 10.3389/fncel.2015.00246

Gadella, T. (2008, December). *FRET and FLIM techniques*. FRET and FLIM Techniques, Volume 33 - 1st Edition. Retrieved August 14, 2022, from https://www.elsevier.com/books/fret-and-flim-techniques/gadella/978-0-08-054958-3

Guo, T., Zhang, D., Zeng, Y., Huang, T. Y., Xu, H., & Zhao, Y. (2020, July 16). Molecular and cellular mechanisms underlying the pathogenesis of Alzheimer's disease - molecular neurodegeneration. BioMed Central.

Johnson, CA; Wright, CE; Ghashghaei, HT (December 2017). "Regulation of cytokinesis during corticogenesis: focus on the midbody". FEBS Letters. 591 (24): 4009–4026. doi:10.1002/1873-3468.12676. PMID 28493553.

Jost, A. P.-T., & Waters, J. C. (2019). *Designing a rigorous microscopy experiment: Validating methods and avoiding bias*. Journal of Cell Biology. doi: 10.1083/jcb.201812109

Kamboh, M. I., Demirci, F. Y., Wang, X., Minster, R. L., Carrasquillo, M. M., Pankratz, V. S., ... & Barmada, M. M. (2012). Genome-wide association study of Alzheimer's disease. Translational psychiatry, 2(5), e117-e117.

Kann O, Kovács R. Mitochondria and neuronal activity. Am J Physiol Cell Physiol. 2007 Feb;292(2):C641-57. doi: 10.1152/ajpcell.00222.2006. Epub 2006 Nov 8. PMID: 17092996.

Kinney, J. W., Bemiller, S. M., Murtishaw, A. S., Leisgang, A. M., Salazar, A. M., & Lamb, B. T. (2018). Inflammation as a central mechanism in Alzheimer's disease. *Alzheimer's & dementia (New York, N. Y.)*, *4*, 575–590. https://doi.org/10.1016/j.trci.2018.06.014

Knopman, D.S., Amieva, H., Petersen, R.C. *et al*. Alzheimer disease. Nat Rev Dis Primers 7, 33 (2021). https://doi.org/10.1038/s41572-021-00269-y

Kumar A, Sidhu J, Goyal A, et al. Alzheimer Disease. [Updated 2022 Jun 5]. In: StatPearls [Internet]. Treasure Island (FL): StatPearls Publishing; 2022 Jan-. Available from: https://www.ncbi.nlm.nih.gov/books/NBK499922/

Macdonald PJ, Chen Y, Mueller JD. Chromophore maturation and fluorescence fluctuation spectroscopy of fluorescent proteins in a cell-free expression system. Anal Biochem. 2012 Feb 1;421(1):291-8. doi: 10.1016/j.ab.2011.10.040. Epub 2011 Oct 28. PMID: 22093611; PMCID: PMC3367886.

Mendez M. F. (2017). Early-Onset Alzheimer Disease. *Neurologic clinics*, *35*(2), 263–281. https://doi.org/10.1016/j.ncl.2017.01.005

Merzlyak EM, Goedhart J, Shcherbo D, Bulina ME, Shcheglov AS, Fradkov AF, Gaintzeva A, Lukyanov KA, Lukyanov S, Gadella TWJ, Chudakov DM. Bright

monomeric red fluorescent protein with an extended fluorescence lifetime. Nat Methods. 2007;**4**:555–557.

Moradifard, S., Hoseinbeyki, M., Ganji, S. M., & Minuchehr, Z. (2018). Analysis of microRNA and gene expression profiles in Alzheimer's disease: a meta-analysis approach. Scientific reports, 8(1), 1-17.

Mythreye, K., & Blobe, G. C. (2009). Proteoglycan signaling co-receptors: roles in cell adhesion, migration and invasion. Cellular signalling, 21(11), 1548–1558. https://doi.org/10.1016/j.cellsig.2009.05.001

Palmer, E., Freeman, T.,(2004) Investigation Into the use of C- and N-terminal GFP Fusion Proteins for Subcellular Localization Studies Using Reverse Transfection Microarrays doi:10.1002/cfg.405

Parpura, V., Grubišić, V., & Verkhratsky, A. (2011). Ca2+ sources for the exocytotic release of glutamate from astrocytes. Biochimica et Biophysica Acta (BBA)-Molecular Cell Research, 1813(5), 984-991.

Perez-Alvarez, A., & Araque, A. (2013). Astrocyte-neuron interaction at tripartite synapses. Current drug targets, 14(11), 1220-1224.

Perez, F. P., Bose, D., Maloney, B., Nho, K., Shah, K., & Lahiri, D. K. (2014). Late-onset Alzheimer's disease, heating up and foxed by several proteins: pathomolecular effects of the aging process. *Journal of Alzheimer's disease : JAD*, *40*(1), 1–17. https://doi.org/10.3233/JAD-131544

Peteri, U.-K., Niukkanen, M., Castrén, M. L. (2019). Astrocytes in neuropathologies affecting the frontal cortex. Front. Cell Neurosci. 13, 44. doi: 10.3389/fncel.2019.00044

Picone, P., Nuzzo, D., Caruana, L., Scafidi, V., & Di Carlo, M. (2014, August 20). *Mitochondrial dysfunction: Different routes to alzheimer's disease therapy*. Oxidative Medicine and Cellular Longevity. From https://www.hindawi.com/journals/omcl/2014/780179/

Purves, Dale (2012). Neuroscience (5th ed.). Sinauer Associates. p. 490. ISBN 9780878936953.

Qi, G., Mi, Y., Shi, X., Gu, H., Brinton, R. D., & Yin, F. (2021). ApoE4 Impairs NeuronAstrocyte Coupling of Fatty Acid Metabolism. Cell reports, 34(1), 108572.

Rabinovici G. D. (2019). Late-onset Alzheimer Disease. Continuum (Minneapolis, Minn.), 25(1), 14–33. https://doi.org/10.1212/CON.0000000000000700

Rafatova, S. (2022). *Comparision of entropy and ensemble based feature selection through network analysis of Alzheimer's disease-associated variants* [Master's thesis, Middle East Technical University*]*

Rhein V, Eckert A (2007) Effects of Alzheimer's amyloid-beta and tau protein on mitochondrial function—role of glucose metabolism and insulin signalling. Arch Physiol Biochem 113:131–141

Rossi, D., Volterra, A. (2009). Astrocytic dysfunction: insights on the role in neurodegeneration. Brain Res. Bull. 80, 224–232. doi: 10.1016/j.brainresbull.2009.07.012

Sadler, T. (2010). Langman's medical embryology (11th ed.). Philadelphia: Lippincott William & Wilkins. pp. 296–297. ISBN 978-07817-9069-7.

Sariyer I. K. (2013). Transfection of neuronal cultures. *Methods in molecular biology (Clifton, N.J.)*, *1078*, 133–139. https://doi.org/10.1007/978-1-62703-640-5_11

Seppälä, T. T., Nerg, O., Koivisto, A. M., Rummukainen, J., Puli, L., Zetterberg, H., Pyykkö, O. T., Helisalmi, S., Alafuzoff, I., Hiltunen, M., Jääskeläinen, J. E., Rinne, J., Soininen, H., Leinonen, V., & Herukka, S. K. (2012). CSF biomarkers for Alzheimer disease correlate with cortical brain biopsy findings. *Neurology*, *78*(20), 1568–1575. https://doi.org/10.1212/WNL.0b013e3182563bd0

Siracusa, R., Fusco, R., & Cuzzocrea, S. (2019, September 27). Astrocytes: Role and functions in brain pathologies. Frontiers from https://www.frontiersin.org/articles/10.3389/fphar.2019.01114/full

Thevenet, J., De Marchi, U., Domingo, J. S., Christinat, N., Bultot, L., Lefebvre, G., *et al*. (2016). Medium-chain fatty acids inhibit mitochondrial metabolism in astrocytes promoting astrocyte-neuron lactate and ketone body shuttle systems. FASEB J. 30, 1913–1926. doi: 10.1096/fj.201500182

Wang, G., Song, R., Lou, K., Leopizzi, M., Dhamija, R., Muniyan, S., Goodwin, B., Vahidnezhad, H., Miao, L., Zhang, J., McGuire, J., Jiang, X., Anderson, M. E., & Wang, W. (2017). *SPOCK1 promotes the growth of osteosarcoma cells through mTOR-S6K signaling pathway*. Biomedicine & Pharmacotherapy. https://doi.org/10.1016/j.biopha.2017.08.116

Williams, S. Mark (2001). "The Initial Formation of the Nervous System: Gastrulation and Neurulation". Neuroscience. 2nd edition.

APPENDICES

A. Composition of Solutions

Table E: Composition of F-12 Nutrient Mixture (Ham's)

Component	Concentration (mg/L)
Inorganic Salts	
Calcium chloride (Anhydrous)	33.22
Cupric sulfate ($CuSO_4$-$5H_2O$)	0.0025
Ferric sulfate ($FeSO_4$-$7H_2O$)	0.834
Potassium chloride (KCl)	223.60
Magnesium chloride (Anhydrous)	57.22
Sodium chloride (NaCl)	7599.00
Sodium bicarbonate ($NaHCO_3$)	1176.00
Sodium phosphate, dibas (Anhydrous)	142.04
Zinc sulfate ($ZnSO_4$-$7H_2O$)	0.863
Other Components	
D-Glucose	1802.00
Hypoxanthine Na	4.7700
Linoleic Acid	0.084
Lipoic Acid	0.21
Phenol red	1,2000
Putrescine-2HCl	0.161
Sodium Pyruvate	110.00

Thymidine	0.73
Amino Acids	
L-Alanine	8.9000
L-Arginine hydrochloride	211.00
L-Asparagine-H_2O	15.00
L-Aspartic acid	13.30
L-Cysteine-HCl-H_2O	35.12
L-Glutamic acid	14.70
L-Glutamine	146.00
Glycine	7.5000
L-Histidine-HCl-H_2O	20.96
L-Isoleucine	3.9400
L-Leucine	13.1000
L-Lysine hydrochloride	36.50
L-Methionine	4.4800
L-Phenylalanine	4.9600
L-Proline	34.50
L-Serine	10.5000
L-Threonine	11.9000
L-Tryptophan	2.0400
L-Tyrosine	5.4000
L-Valine	11.7000
Vitamins	
Biotin	0.0073
D-Calcium pantothenate	0.48
Choline chloride	13.96

Folic acid	1.3000
i-Inositol	18.00
Niacinamide	0.037
Pyridoxine hydrochloride	0.062
Riboflavin	0.038
Thiamine hydrochloride	0.34
Vitamin B12	1.3600

Table F: Composition of MEM-Eagle

Components	Concentration (mg/L)
Inorganic Salts	
Calcium Chloride (CaCl2) (Anhyd.)	200.00
Potassium Chloride (KCl)	400.00
Magnesium Sulfate (MgSO4)	97.67
Sodium Chloride (NaCl)	6800.00
Sodium Bicarbonate (NaHCO3)	2200.00
Sodium Phosphate-H2O (NaH2PO4-H2O)	140.00
Other Components	
D-Glucose	1000.00
Phenol Red	10.00
AMINO ACIDS:	
L-Arginine-HCl	126.00
L-Cystine	24.00
L-Histidine-HCl-H2O	42.00
L-Isoleucine	52.00
L-Leucine	52.00
L-Lysine-HCl	72.50
L-Methionine	15.00

L-Phenylalanine	32.00
L-Threonine	48.00
L-Tryptophan	10.00
L-Tyrosine	36.00
L-Valine	46.00
Vitamins	
D-Ca Pantothenate	1.00
Choline Chloride	1.00
Folic Acid	1.00
i-Inositol	2.00
Niacinamide	1.00
Pyridoxal HCl	1.00
Riboflavin	0.10
Thiamine HCl	1.00

Table G: Composition of DMEM with High Glucose

Components	**Concentration (mg/L)**
Amino Acids	
Glycine	30
L-Arginine.HCl	84
L-Cysteine.2HCl	63
L-Glutamine	580
L-Histidine Hydrochloride-H2O	42
L-Isoleucine	105
L-Leucine	105
L-Lysine.HCl	146
L-Methionine	30
L-Phenylalanine	66

L-Serine	42
L-Threonine	95
L-Tryptophan	16
L-Tyrosine	72
L-Valine	94
Vitamins	
Choline Chloride	4
D-Calcium Pantothenate	4
Folic Acid	4
Niacinamide	4
Pyridoxine Hydrochloride	4
Riboflavin	0,4
Thiamine Hydrochloride	4
I-Inistol	7.2
Inorganic Salts	
Calcium Chloride	264
Ferric Nitrate	0.1
Magnesium Sulfate	200
Potassium Chloride	400
Sodium Bicarbonate	3700
Sodium Chloride	6400
Sodium Phosphate Monobasic	141
Other Compotents	
D-Glucose(dexrose)	4500
Phenol Red	15
Sodium Pyruvate	110

Table H: Composition of 1X PBS Solution

Component	**Amount**
NaCl	8 g/L
KCl	0.2 g/L
Na_2HPO_4	1.44 g/L
KH_2PO_4	0.24 g/L

All ingredients were dissolve into 1 litre deionieze steril water and pH is adjuste to 7.4 .

Table I: Composition of Luria Bertani (LB) Medium

Component	**Amount**
Tryptone	10 g/L
NaCl	5 g/L
Yeast Extract	5 g/L

All ingredients were dissolve into distilled water and the pH is adjuste to 7.0 . 20 g/L agar was added for LB Agar plate preperation.

Table J: Composition of 1X NEB CutSmart Buffer

Component	**Amount**
Potassium Acetate	50 mM
Tris-Acetate	20 mM
Magnesium Acetate	10 mM
BSA	10 µg/mL

Table K: T4DNA Ligase Reaction Buffer

Component	Amount
Tris-HCl	50 mM
MgCl2	10 mM
ATP	1 mM
Dithiothreitol	10 mM

Table L: Composition of TFBI and TFBII

TFBI	**Final Concentration**	**Prepared Stock**	**For 100mL solution taken from prepared stock**
KOAc	30mM	300mM	10mL
RBCl	100mM	1000mM	10mL
CaCl2	10mM	1000mM	1mL
MnCl2	50mM	1000mM	5mL
Glycerol	15%	87%	17.2mL
TFB2	**Final Concentration**	**Prepared Stock**	**For 10mL Solution taken from prepared stock**
MOPS/PIPES	10mM	1000mM	0.1mL
$RbCl_2$	10mM	1000mM	0.1mL
$CaCl_2$	75mM	1000mM	0.75mL
Glycerol	15%	87%	1.7mL

The TFBI solution completed to 100mL and the TFBII solution completed to 10mL with using deionized water and the pH adjusted to 5.8. Then, the solutions were filtered through 0.22 μm filter.

B. Primers

C-terminal tagging primers:

EGFP-SPOCK1-F:

GCAACTCGGACTAGGGGACCCGGGCCGGCCCCCAAGATG**GTGAGCAAGGGCGAGGAG**

EGFP-SPOCK1-R:

CGCCGCGGCGGCCGCCGCCAACACCGCGATCGCCGGCTTGTACAGCTCGTCCATGCC
G

SPOCK1ns-BamHI-R (GACAAAGAGGATGAGGTCGGGTACATATGG**GGATCC)**

GTTGTTGGATCCCCATATGTACCCGACCTCATCCTCTTTGTC

31st Position EGFP/mCherry tagged SPOCK1 Primers

Spock-31-EGFP-F:

GTCGAGAGCCGGCACCTGGACGCGCTCGCCGGAGGCGCG**GTGAGCAAGGGCGAGGAG**

Spock-31-EGFP-R:
(**CGGCATGGACGAGCTGTACAAG**GGCCCCAACCACGGCAATTTCCTAGACAATGACC
AG)

CTGGTCATTGTCTAGGAAATTGCCGTGGTTGGGGCCCTTGTACAGCTCGTCCATGCC
G

C. Plasmid Maps

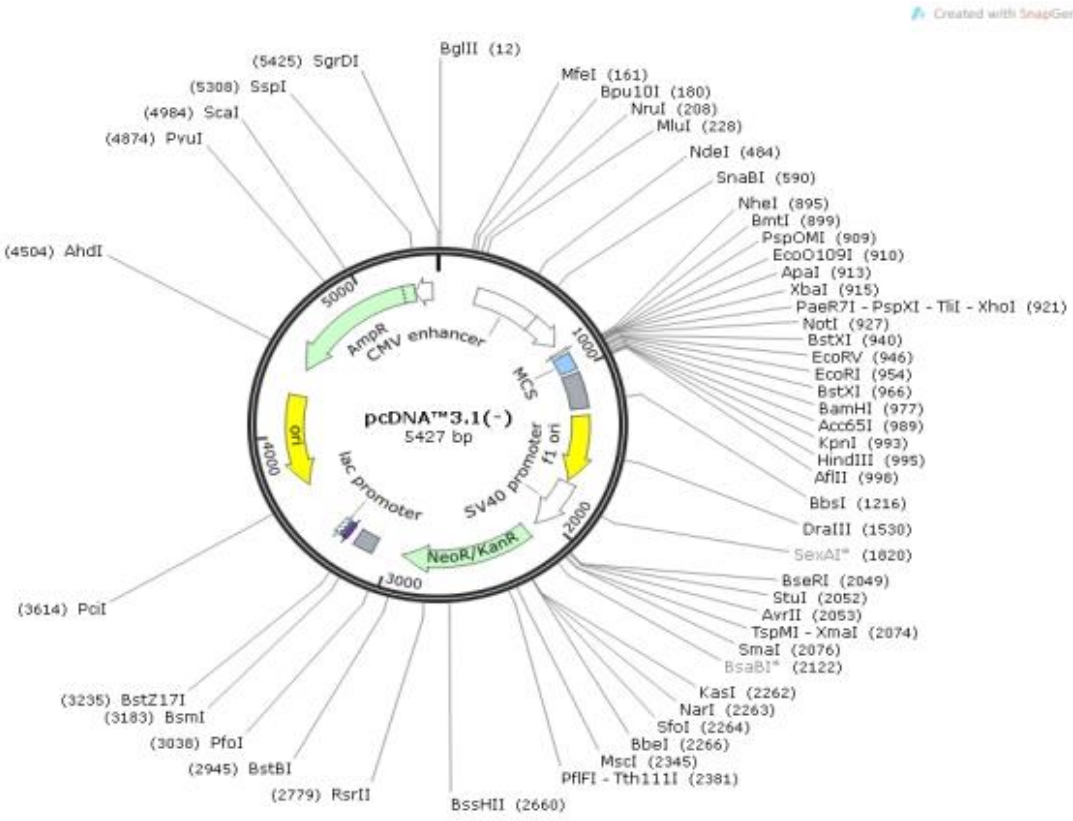

Figure 6.1: Plasmid Map of pcDNA 3.1(-) (from SnapGene)

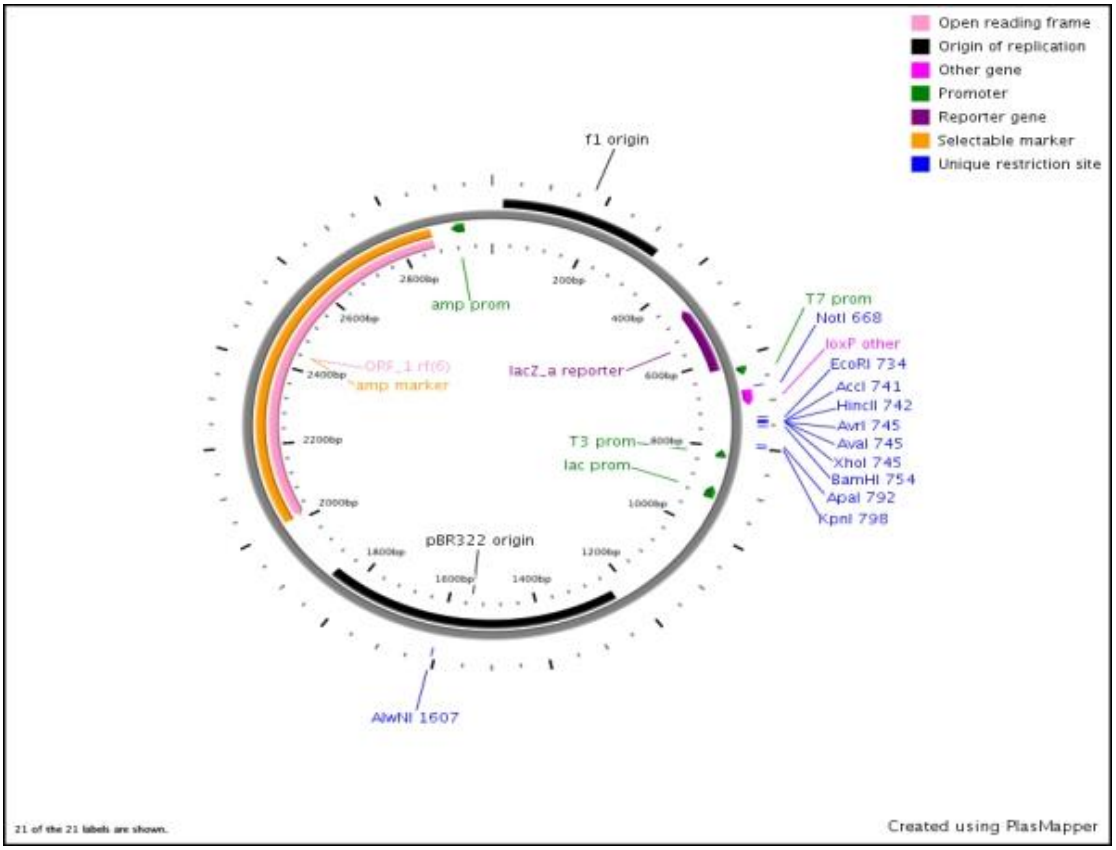

Figure 6.2: Plasmid Map of pBlueScriptR (from DNAform)

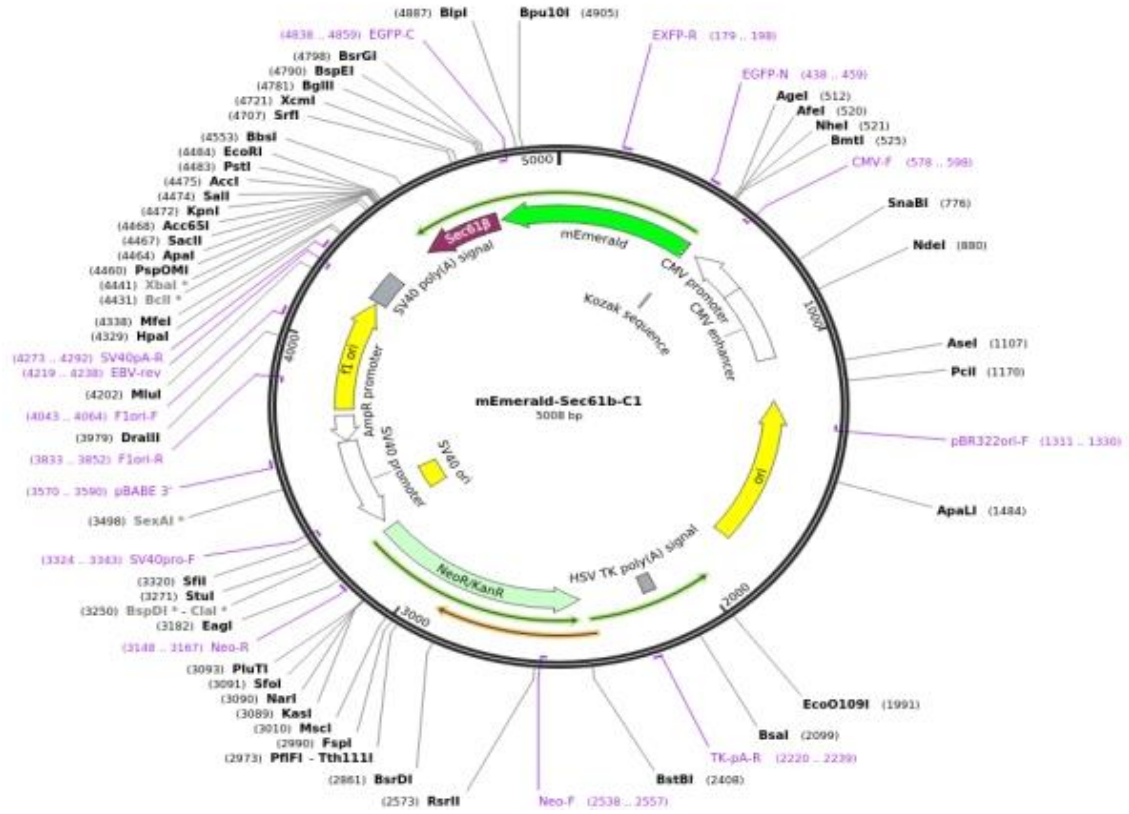

Figure 6.3:Plasmid Map of mEmerald-Sec61b-C1 ER Organel Marker (from SnapGene)

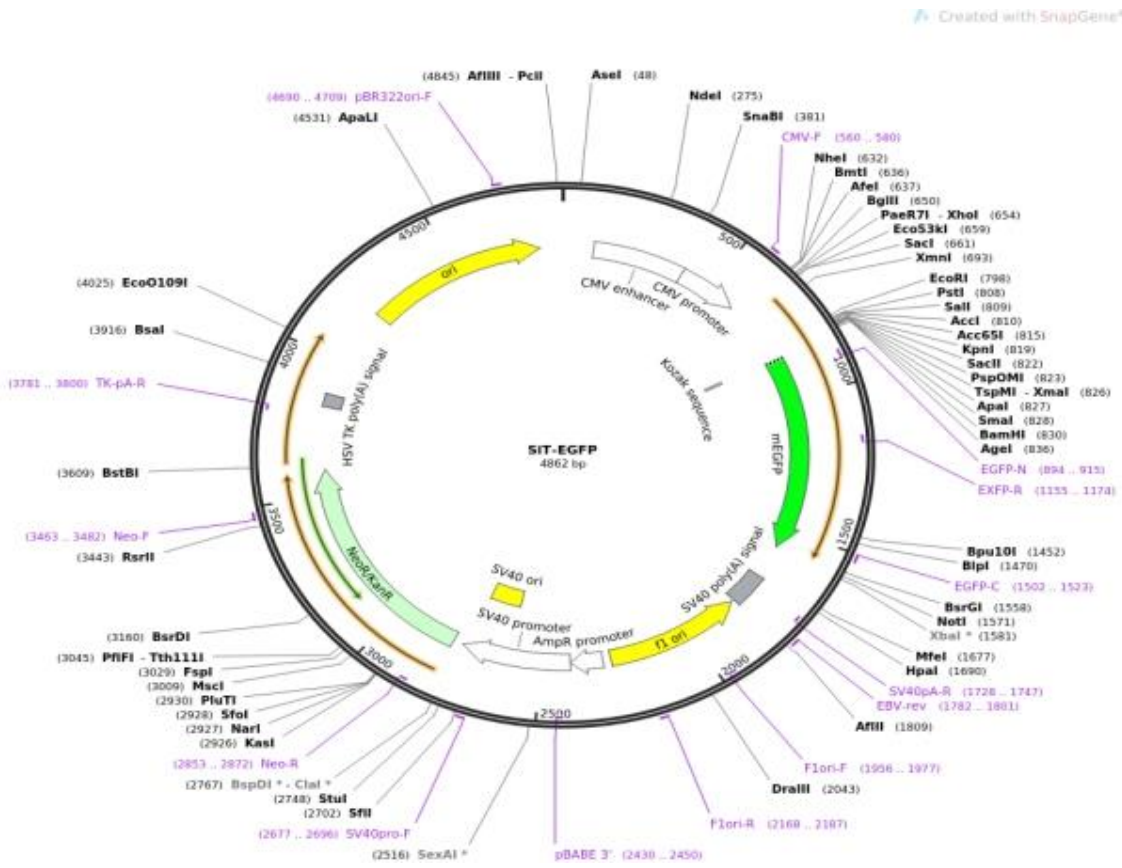

Figure 6.4: Plasmid Map of SiT-EGFP Golgi Organel(from SnapGene)

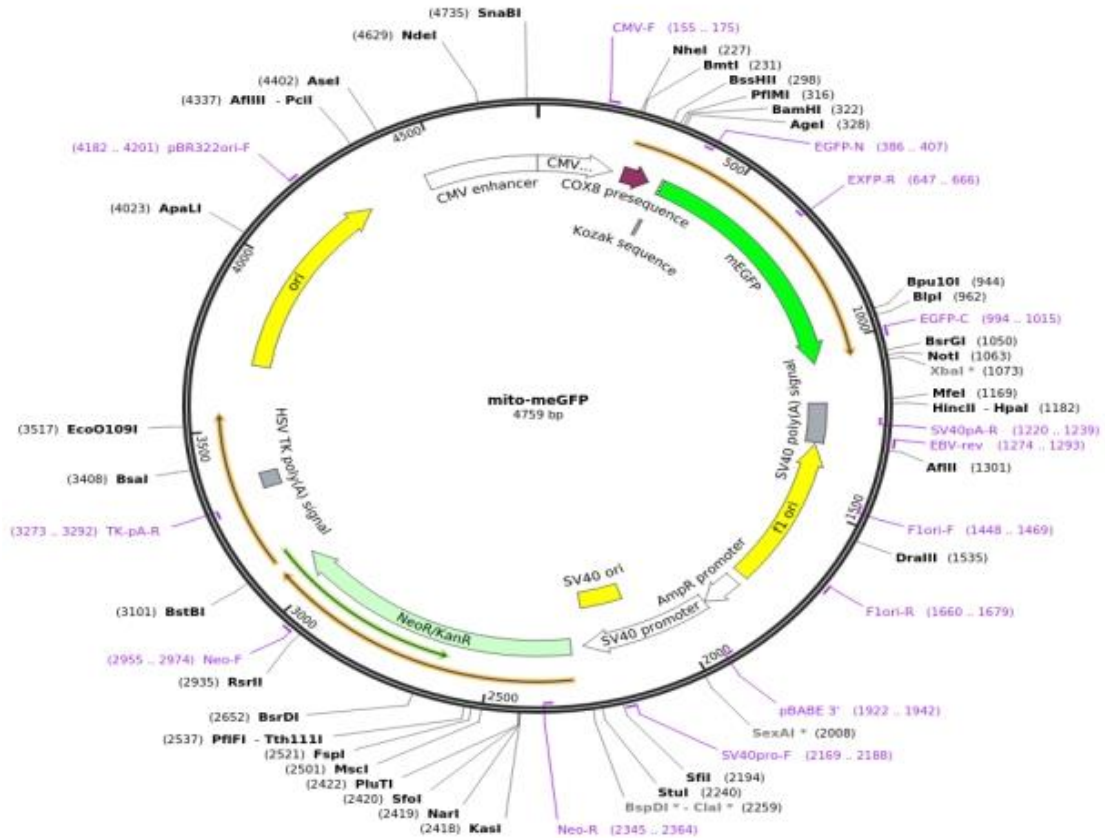

Figure 6.5: Plasmid Map of mito-meGFP Mitochondria Organel Marker (from SnapGene).

D. Sequencing Data of Tagged Constructs

D1. C-Term mCherry Tagged SPOCK1 Sequence

TGGCTGGCACTAGAAGGCACAGTCGAGGCTGATCAGCGGTTTAAACTTAAGCTTGGT
ACCTTACTTGTACAGCTCGTCCATGCCGCCGGTGGAGTGGCGGCCCTCGGCGCGTTC
GTACTGTTCCACGATGGTGTAGTCCTCGTTGTGGGAGGTGATGTCCAACTTGATGTT
GACGTTGTGGGCGCCGGGCAGCTGCACGGGCTTCTTGGCCTTGTAGGTGGTCTTGAC
CTCAGCGTCGTAGTGGCCGCCGTCCTTCAGCTTCAGCCTCTGCTTGATCTCGCCCTT
CAGGGCGCCGTCCTCGGGGTACATCCGCTCGGAGGAGGCCTCCCAGCCCATGGTCTT
CTTCTGCATTACGGGGCCGTCGGAGGGGAAGTTGGTGCCGCGCAGCTTCACCTTGTA
GATGAACTCGCCGTCCTGCAGGGAGGAGTCCTGGGTCACGGTCACCACGCCGCCGTC
CTCGAAGTTCATCACGCGCTCCCACTTGAAGCCCTCGGGGAAGGACAGCTTCAAGTA
GTCGGGGATGTCGGCGGGGTGCTTCACGTAGGCCTTGGAGCCGTACATGAACTGAGG
GGACAGGATGTCCCAGGCGAAGGGCAGGGGGCCACCCTTGGTCACCTTCAGCTTGGC
GGTCTGGGTGCCCTCGTAGGGGCGGCCCTCGCCCTCGCCCTCGATCTCGAACTCGTG
GCCGTTCACGGAGCCCTCCATGTGCACCTTGAAGCGCATGAACTCCTTGATGATGGC
CATGTTATCCTCCTCGCCCTTGCTCACCATGGATCCCCATATGTACCCGACCTCATC
CTCTTTGTCATCATCCTCATCCTCATCATCCTCTGTCACGGCTCGGGTGTGCACCCT
CAGCTTCCCCTCTTTGTCCTTTGGTCCCAGCTCCCGTTCATATTCTAGGTCATCCAG
CAGGACCACGGACCCACCACTGCCAAAATCCCCTGAGGTTTCCTGCTCCTCTTCACA
GCTCACAGCACCCTGTTTCCTGGAGCCAGCCAACTCATTCCCATATTTGTCCACACA
C C A G N A C T G C C T C G T G C T G C C G T G G C A C T G G N T G G C T T G T

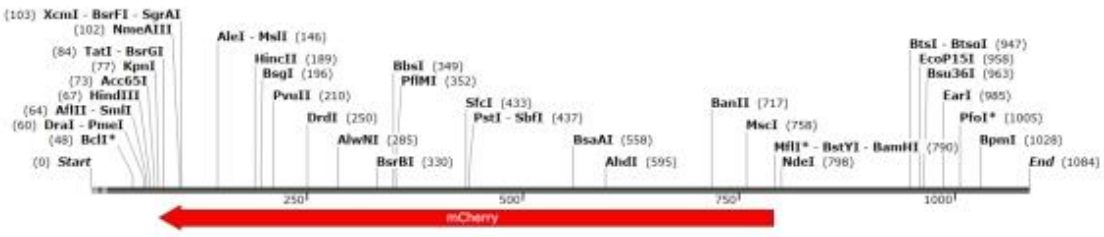

Figure 6.6: Linear Map for mCherry sequence.

D2. C-Term mEGFP Tagged SPOCK1 Sequence

GNTGGCTGGCACTAGAAGGCACAGTCGAGGCTGATCAGCGGTTTAAACTTAAGCTTG
GTACCTTACTTGTACAGCTCGTCCATGCCGAGAGTGATCCCGGCGGCGGTCACGAAC
TCCAGCAGGACCATGTGATCGCGCTTCTCGTTGGGGTCTTTGCTAAGCTTGGACTGG
GTGCTCAGGTAGTGGTTGTCGGGCAGCAGCACGGGGCCGTCGCCGATGGGGGTGTTC
TGCTGGTAGTGGTCGGCGAGCTGCACGCTGCCGTCCTCGATGTTGTGGCGGATCTTG
AAGTTCACCTTGATGCCGTTCTTCTGCTTGTCGGCCATGATATAGACGTTGTGGCTG
TTGTAGTTGTACTCCAGCTTGTGCCCCAGGATGTTGCCGTCCTCCTTGAAGTCGATG
CCCTTCAGCTCGATGCGGTTCACCAGGGTGTCGCCCTCGAACTTCACCTCGGCGCGG
GTCTTGTAGTTGCCGTCGTCCTTGAAGAAGATGGTGCGCTCCTGGACGTAGCCTTCG
GGCATGGCGGACTTGAAGAAGTCGTGCTGCTTCATGTGGTCGGGGTAGCGGCTGAAG
CACTGCACGCCGTAGGTCAGGGTGGTCACGAGGGTGGGCCAGGGCACGGGCAGCTTG
CCGGTGGTGCAGATGAACTTCAGGGTCAGCTTGCCGTAGGTGGCATCGCCCTCGCCC
TCGCCGGACACGCTGAACTTGTGGCCGTTTACGTCGCCGTCCAGCTCGACCAGGATG
GGCACCACCCCGGTGAACAGCTCCTCGCCCTTGCTCACCATGGATCCCCATATGTAC
CCGACCTCATCCTCTTTGTCATCATCCTCATCCTCATCATCCTCTGTCACGGCTCGG
GTGTGCACCCTCAGCTTCCCCTCTTTGTCCTTTGGTCCCAGCTCCCGTTCATATTCT
AGGTCATCCAGCAGGACCACGGACCCACCACTGCCAAAATCCCCTGAGGTTTCCTGC
TCCTCTTCACAGCTCACAGCACCCTGTTTCCTGGAGCCAGCCAACTCATTCCCATAT
T T G T C C A C C C C N A A C A C T G C C C C G T G C T G C C G T G G C

A206K EGFP mutant produces the monomeric variant mEGFP.

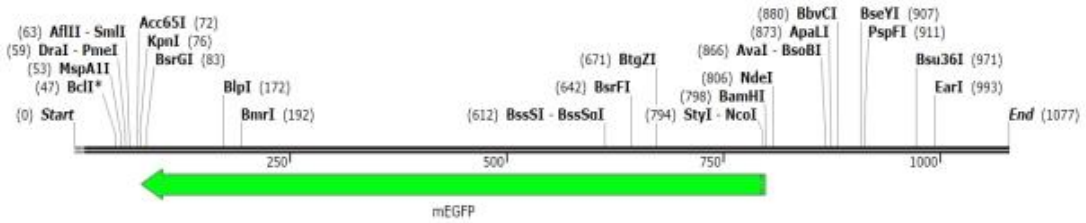

Figure 6.7: Linear Map for mEGFP sequence.

D3. 31st Position mCherry Tagged SPOCK1 Sequence

NNNNNCNTNGNNNNNNNNNNCNNCTGCTTACTGGCTTATCGAAATTAATACGACTC
ACTATAGGGAGACCCAAGCTGGCTAGCGTTTAAACGGGCCCTCTAGAATGCCGGCGA
TCGCGGTGTTGGCGGCGGCCGCCGCGGCGTGGTGCTTCCTCCAAGTCGAGAGCCGGC
ACCTGGACGCGCTCGCCGGAGGCGCGGTGAGCAAGGGCGAGGAGGATAACATGGCCA
TCATCAAGGAGTTCATGCGCTTCAAGGTGCACATGGAGGGCTCCGTGAACGGCCACG
AGTTCGAGATCGAGGGCGAGGGCGAGGGCCGCCCCTACGAGGGCACCCAGACCGCCA
AGCTGAAGGTGACCAAGGGTGGCCCCCTGCCCTTCGCCTGGGACATCCTGTCCCCTC
AGTTCATGTACGGCTCCAAGGCCTACGTGAAGCACCCCGCCGACATCCCCGACTACT
TGAAGCTGTCCTTCCCCGAGGGCTTCAAGTGGGAGCGCGTGATGAACTTCGAGGACG
GCGGCGTGGTGACCGTGACCCAGGACTCCTCCCTGCAGGACGGCGAGTTCATCTACA
AGGTGAAGCTGCGCGGCACCAACTTCCCCTCCGACGGCCCCGTAATGCAGAAGAAGA
CCATGGGCTGGGAGGCCTCCTCCGAGCGGATGTACCCCGAGGACGGCGCCCTGAAGG
GCGAGATCAAGCAGAGGCTGAAGCTGAAGGACGGCGGCCACTACGACGCTGAGGTCA
AGACCACCTACAAGGCCAAGAAGCCCGTGCAGCTGCCCGGCGCCCACAACGTCAACA
TCAAGTTGGACATCACCTCCCACAACGAGGACTACACCATCGTGGAACAGTACGAAC
GCGCCGAGGGCCGCCACTCCACCGGCGGCATGGACGAGCTGTACAAGGGCCCCAACC
ACGGCAATTTCCTAGACAATGACCAGTGGCTGAGCACCGTCTCCCAGTACGACCGGG
ACAAGTACTGGAACCGCTTTCGAGACGATGATTATTTCAGAAACTGGAATCCCAACA
AGCCCTTTGACAAAGCCCTGGACCCATCCAAGGACCCCTGCCTGAAGGTAAAATGCA
GCCCTCCAAAGTGTGTGTGACCCAGGACTACCAANCCGCCCTGTGTNTCACCGCAAG
CCCTGCTCCCCAGCAAAAGAAGGGAACNGGCCCAGAACCTGGGTTGGACTTCGATTT
GGTCAGTGCAACCCTGTCCCGGGCCAATCAGCCTGGTCTGCGGNTCAAAGGCCCC

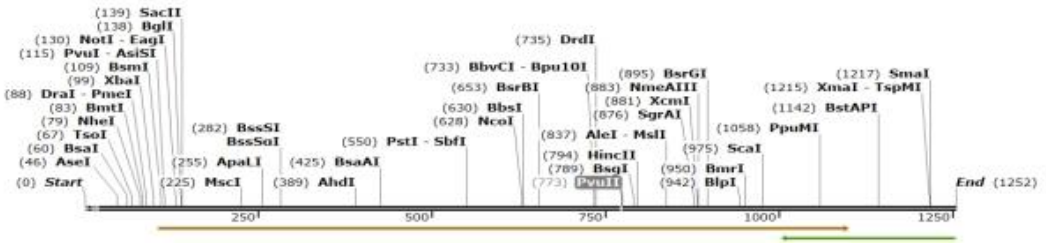

Figure 6.8:Linear Map for 31st position mCherry tagged SPOCK1 sequence.

D4. 31st Position mEGFP Tagged SPOCK1 Sequence

NNNNNNNNNNNNGCTACTAGANANNCACTGCTTACTGGCTTATCGAAATTAATACGA
CTCACTATAGGGAGACCCAAGCTGGCTAGCGTTTAAACGGGCCCTCTAGAATGCCGG
CGATCGCGGTGTTGGCGGCGGCCGCCGCGGCGTGGTGCTTCCTCCAAGTCGAGAGCC
GGCACCTGGACGCGCTCGCCGGAGGCGCGGTGAGCAAGGGCGAGGAGCTGTTCACCG
GGGTGGTGCCCATCCTGGTCGAGCTGGACGGCGACGTAAACGGCCACAAGTTCAGCG
TGTCCGGCGAGGGCGAGGGCGATGCCACCTACGGCAAGCTGACCCTGAAGTTCATCT
GCACCACCGGCAAGCTGCCCGTGCCCTGGCCCACCCTCGTGACCACCCTGACCTACG
GCGTGCAGTGCTTCAGCCGCTACCCCGACCACATGAAGCAGCACGACTTCTTCAAGT
CCGCCATGCCCGAAGGCTACGTCCAGGAGCGCACCATCTTCTTCAAGGACGACGGCA
ACTACAAGACCCGCGCCGAGGTGAAGTTCGAGGGCGACACCCTGGTGAACCGCATCG
AGCTGAAGGGCATCGACTTCAAGGAGGACGGCAACATCCTGGGGCACAAGCTGGAGT
ACAACTACAACAGCCACAACGTCTATATCATGGCCGACAAGCAGAAGAACGGCATCA
AGGTGAACTTCAAGATCCGCCACAACATCGAGGACGGCAGCGTGCAGCTCGCCGACC
ACTACCAGCAGAACACCCCCATCGGCGACGGCCCCGTGCTGCTGCCCGACAACCACT
ACCTGAGCACCCAGTCCAAGCTTAGCAAAGACCCCAACGAGAAGCGCGATCACATGG
TCCTGCTGGAGTTCGTGACCGCCGCCGGGATCACTCTCGGCATGGACGAGCTGTACA
AGGGCCCCAACCACGGCAATTTCCTAGACAATGACCAGTGGCTGAGCACCGTCTCCC
AGTACGACCGGGACAAGTACTGGAACCGCTTTCGAGACGATGATTATTTCAGAAACT
GGAATCCCAACAAGCCCTTTGACAAAGCCCTGGACCCATCCAAGGACCCCTGCCTGA
AGGTAAAATGCAGCCCTCCAAAGTGGGTGTGACCCAGACTACCAAACGCCCTGTGTG
TCACCGCAAGCACTGCTCCCAGGCAAAGAAGGGGAACGGGCCCAAAAACCTGGGTTG
G A C C T T C A A A T T G G T C A A T G C A A C C C T G T C C G T G G

A206K EGFP mutant produces the monomeric variant mEGFP.

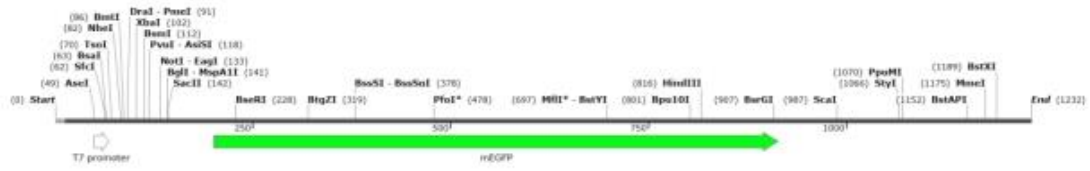

Figure 6.9: Linear Map for 31st position EGFP tagged SPOCK1 sequence.

E. Mitochondria Marker mScarlet Transfection

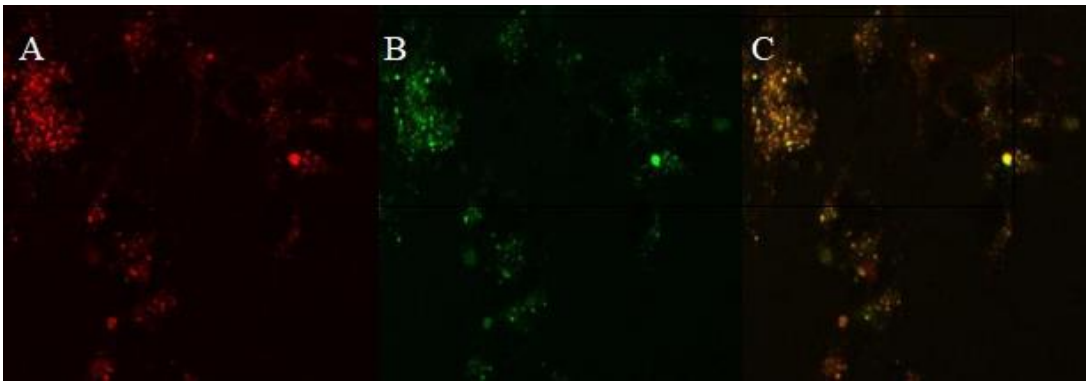

Figure 6.10 : mScarlet single transfection on SH-SY5Y A) mScarlet(Red) single transfection on SH-SY5Y at 561 nm with 63x. B) Mitochondria Marker mScarlet(Red) single transfection on SH-SY5Y at 488 nm with objective C) Merge of A & B.

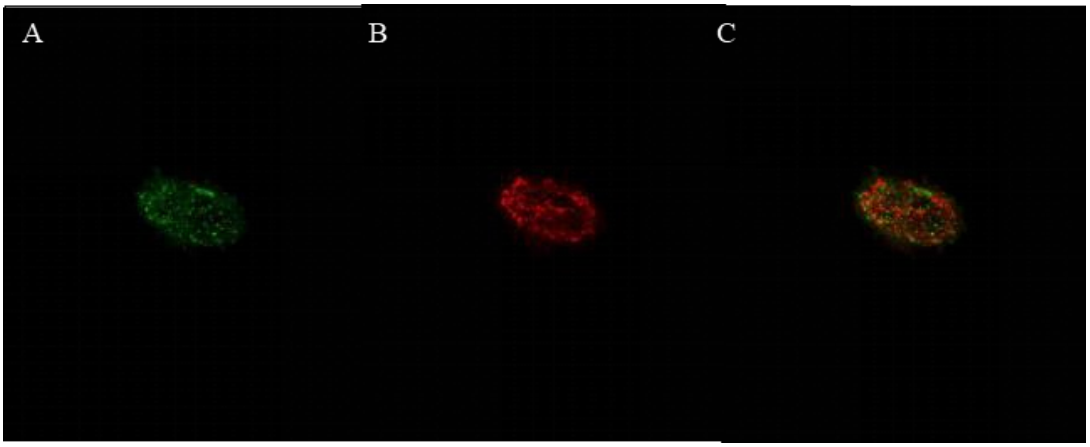

Figure 6.11 : mScarlet vs EGFP SPOCK1 on SVG p12 A) EGFP SPOCK1 (Green) transfection on SVG p12 cell at 488 nm with 63x B) Mitochondria Marker mScarlet (Red) transfection on SVG p12 cell at 561 nm with 63x C) Merge of A & B,